Optimistic limits of the colored Jones invariants

Jinseok Cho and Jun Murakami

October 25, 2010

Abstract

We show that the optimistic limits of the colored Jones invariants of the hyperbolic knots coincide with the minus of the optimistic limit of the Kashaev invariants modulo $2\pi^2$.

1 Main Results

Kashaev conjectured the following relation in [5] :

$$\mathrm{vol}(L) = 2\pi \lim_{N\to\infty} \frac{\log|\langle L\rangle_N|}{N},$$

where L is a hyperbolic link, $\mathrm{vol}(L)$ is the hyperbolic volume of $S^3 - L$, $\langle L\rangle_N$ is the N-th Kashaev invariant. After that, the generalized conjecture was proposed in [12] that

$$i(\mathrm{vol}(L) + i\,\mathrm{cs}(L)) \equiv 2\pi i \lim_{N\to\infty} \frac{\log\langle L\rangle_N}{N} \pmod{\pi^2},$$

where $\mathrm{cs}(L)$ is the Chern-Simons invariant of $S^3 - L$ defined in [7].

The calculation of the actual limit of the Kashaev invariant is very hard, and only several cases are known. On the other hand, while proposing the conjecture, Kashaev used some formal approximation to predict the actual limit. His formal approximation was formulated as *optimistic limit* by H. Murakami in [9]. This method can be summarized by the following way. At first, we fix an expressed equation of $\langle L\rangle_N$ and then apply the following *formal substitution*

$$\begin{aligned}
(q)_k &\sim \exp\left\{\frac{N}{2\pi i}\left(-\mathrm{Li}_2(q^k) + \frac{\pi^2}{6}\right)\right\}, \qquad (1)\\
(q^{-1})_k &\sim \exp\left\{\frac{N}{2\pi i}\left(\mathrm{Li}_2(q^{-k}) - \frac{\pi^2}{6}\right)\right\},\\
q^{kl} &\sim \exp\left\{\frac{N}{2\pi i}\left(\log q^k \cdot \log q^l\right)\right\},
\end{aligned}$$

to the equation, where $q=\exp(2\pi i/N)$, $(q)_k=\prod_{n=1}^{k}(1-q^n)$ and $\mathrm{Li}_2(z)=-\int_0^z\frac{\log(1-t)}{t}dt$ for $z\in\mathbb{C}$. Then, by substituting each q^k to a complex variable z, we obtain a potential function $\exp\left\{\frac{N}{2\pi i}V(\ldots,z,\ldots)\right\}$. Finally, let

$$V_0(\ldots,z,\ldots):=V-\sum_z\left(z\frac{\partial V}{\partial z}\right)\log z$$

and evaluate an *appropriate solution* of the equations $\left\{\exp\left(z\frac{\partial V}{\partial z}\right)=1\right\}$ to V_0. Then, the resulting complex number is called the optimistic limit and denoted by $2\pi i \underset{N\to\infty}{\text{o-lim}}\frac{\log\langle L\rangle_N}{N}$.

For example, the optimistic limit of the Kashaev invariant of the 5_2 knot was calculated in [5] and [13] as follows. By the formal substitution,

$$\langle 5_2\rangle_N=\sum_{k\leq l}\frac{(q)_l^2}{(q^{-1})_k}q^{-k(l+1)}\sim\exp\left\{\frac{N}{2\pi i}\left(-2\mathrm{Li}_2(q^l)-\mathrm{Li}_2(\frac{1}{q^k})-\log q^l\log q^k+\frac{\pi^2}{2}\right)\right\}.$$

By substituting $z=q^l$ and $u=q^k$, we obtain

$$V(z,u)=-2\mathrm{Li}_2(z)-\mathrm{Li}_2(\frac{1}{u})-\log z\log u+\frac{\pi^2}{2},$$

and

$$V_0(z,u)=V(z,u)-\left(z\frac{\partial V}{\partial z}\right)\log z-\left(u\frac{\partial V}{\partial u}\right)\log u.$$

For a choice of a solution $(z_0,u_0)=(0.3376...-0.5623...i,\ 0.1226...+0.7449...i)$ of the equations $\left\{\exp\left(z\frac{\partial V}{\partial z}\right)=1,\ \exp\left(u\frac{\partial V}{\partial u}\right)=1\right\}$, the optimistic limit becomes

$$2\pi i \underset{N\to\infty}{\text{o-lim}}\frac{\log\langle 5_2\rangle_N}{N}=V_0(z_0,u_0)=3.0241...+2.8281...i,$$

and it coincides with $i(\mathrm{vol}(5_2)+i\,\mathrm{cs}(5_2))$ modulo π^2.

As seen above, the optimistic limit depends on the expressed equation and the choice of the solution, so it is not well-defined. Although the optimistic limit is not yet proved to give the actual limit of the Kashaev invariant, Yokota made a very useful way to determine the optimistic limit by fixing a potential function, which depends only on the knot diagram, and by choosing unique solution corresponding to Yokota triangulation of the knot complement in [20] and [19]. Furthermore, he showed in [19] that the optimistic limit determined by his method becomes

$$2\pi i \underset{N\to\infty}{\text{o-lim}}\frac{\log\langle K\rangle_N}{N}\equiv(\mathrm{vol}(K)+i\mathrm{cs}(K))\pmod{\pi^2}\tag{2}$$

for a hyperbolic knot K with a fixed diagram.

On the other hand, it was proved in [11] that

$$J_L(N;\exp\frac{2\pi i}{N})=\langle L\rangle_N,$$

where $J_L(N;x)$ is the N-th colored Jones invariant of the link L with a complex variable x. Therefore, it is natural to expect that the optimistic limit of the colored Jones invariant also gives the volume and the Chern-Simons invariant. Although it looks trivial, due to the ambiguity of the definition of the optimistic limit, only few results were known. It was numerically confirmed for few examples in [12], actually proved only for the volume part of two bridge links in [13] and for the Chern-Simons part of twist knots in [2]. The purpose of this article is to propose a method to determine the optimistic limit of the colored Jones invariant and then prove the following relation :

$$2\pi i \underset{N\to\infty}{\text{o-lim}} \frac{\log\langle K\rangle_N}{N} \equiv -2\pi i \underset{N\to\infty}{\text{o-lim}} \frac{\log J_K(N;\exp\frac{2\pi i}{N})}{N} \pmod{2\pi^2}.$$

The exact statement is the following theorem.

Theorem 1.1 *Let K be a hyperbolic knot with a fixed diagram satisfying Yokota's Assumptions 1–6 in [19]. Also let $V(z_1,\ldots,z_g)$ be the Yokota's potential function of the knot diagram. Assume the hyperbolicity equation $\mathcal{H}_1 := \left\{\exp\left(z_k\frac{\partial V}{\partial z_k}\right) = 1 \mid k=1,\ldots,g\right\}$ has an essential solution and let $(z_1^{(0)},\ldots,z_g^{(0)})$ be the geometric solution. Then there exist another potential functions $W(w_1,\ldots,w_m)$ and*

$$W_0(w_1,\ldots,w_m) := W - \sum_{l=1}^{m}\left(w_l\frac{\partial W}{\partial w_l}\right)\log w_l$$

satisfying

1. *$\mathcal{H}_2 := \left\{\exp\left(w_l\frac{\partial W}{\partial w_l}\right) = 1 \mid l=1,\ldots,m\right\}$ becomes the hyperbolicity equations of Thurston triangulation, which corresponds to the colored Jones invariant,*

2. *For any essential solution $(z_1,\ldots,z_g)$ of $\mathcal{H}_1$, there exists an essential solution $(w_1,\ldots,w_m)$ of $\mathcal{H}_2$ satisfying*

$$V_0(z_1,\ldots,z_g) \equiv -W_0(w_1,\ldots,w_m) \pmod{4\pi^2}.$$

3. *There exists the geometric solution $(w_1^{(0)},\ldots,w_m^{(0)})$ satisfying*

$$\begin{aligned} V_0(z_1^{(0)},\ldots,z_g^{(0)}) &= 2\pi i \underset{N\to\infty}{\text{o-lim}} \frac{\log\langle K\rangle_N}{N} \\ &\equiv -W_0(w_1^{(0)},\ldots,w_n^{(0)}) = -2\pi i \underset{N\to\infty}{\text{o-lim}} \frac{\log J_K(N;\exp\frac{2\pi i}{N})}{N} \pmod{2\pi^2} \\ &\equiv i(\mathrm{vol}(K) + i\,\mathrm{cs}(K)) \pmod{\pi^2}. \end{aligned}$$

The meaning of Yokota's assumptions, Yokota's potential function V, the hyperbolicity equations, the essential solution and the geometric solution will be explained in later sections. The proof of Theorem 1.1 will be in Section 4 and Section 5.

We remark that the assumptions of Theorem 1.1 are the same one appeared in [19], which are needed to guarantee the identity (2). Also we remark that this result suggests the possibility of the well-definedness of the optimistic limit modulo $2\pi^2$.[1] An interesting fact is that the coincidence of two optimistic limits holds modulo $2\pi^2$, not modulo π^2. We expect the optimistic has more information than the volume and the Chern-Simons invariant of the cusped manifold.

Using Theorem 1.1, we obtain the colored Jones invariant version of Corollary 1.4 of [1] as follows.

Corollary 1.2 *Let* $\mathrm{w} := (w_1, \ldots, w_m)$ *be any essential solution of* $\mathcal{H}_2$ *and* $\rho_{\mathrm{w}} : \pi_1(S^3 - K) \to \mathrm{PSL}(2, \mathbb{C})$ *be the parabolic representation induced by* w*. Then*

$$W_0(\mathrm{w}) \equiv -i(\mathrm{vol}(\rho_{\mathrm{w}}) + i\,\mathrm{cs}(\rho_{\mathrm{w}})) \pmod{\pi^2}$$

where $\mathrm{vol}(\rho_{\mathrm{w}}) + i\,\mathrm{cs}(\rho_{\mathrm{w}})$ *is the complex volume of* ρ_{w} *defined in [21]. Furthermore, for any essential solution* w *and the geometric solution* $\mathrm{w}^{(0)} := (w_1^{(0)}, \ldots, w_m^{(0)})$*, the following inequality holds:*

$$|\mathrm{Im} W_0(\mathrm{w})| \leq -\mathrm{Im} W_0(\mathrm{w}^{(0)}) = \mathrm{vol}(K).$$

Proof. From Observation 2.1 in Section 2, we know there are one to one correspondence between the essential solutions of $\mathcal{H}_1$ and the essential solutions of $\mathcal{H}_2$. Let $\mathrm{z} := (z_1, \ldots, z_g)$ be the essential solution of $\mathcal{H}_1$ corresponding to w. Then, by Observation 2.1, we know $\rho_{\mathrm{w}} = \rho_{\mathrm{z}}$. Also, by Theorem 1.1.2, we know $W_0(\mathrm{w}) \equiv -V_0(\mathrm{z}) \pmod{4\pi^2}$.

Yokota proved

$$V_0(\mathrm{z}^{(0)}) \equiv i(\mathrm{vol}(K) + i\,\mathrm{cs}(K)) \pmod{\pi^2},$$

in [19] using Zickert's formula of [21], but the formula also holds for any parabolic representation ρ_{z} induced by an essential solution z of $\mathcal{H}_1$. Therefore, Yokota's proof also implies

$$V_0(\mathrm{z}) \equiv -i(\mathrm{vol}(\rho_{\mathrm{z}}) + i\,\mathrm{cs}(\rho_{\mathrm{z}})) \pmod{\pi^2},$$

for any essential solution z of $\mathcal{H}_1$.

It is a well-known fact that the hyperbolic volume is the maximal value of volumes of all possible $\mathrm{PSL}(2, \mathbb{C})$ representations. (For the proof and the details, see [4].) Therefore, we obtain the result.

□

Using Gromov-Thurston-Goldman rigidity in [3] and Corollary 1.2, we can calculate the complex volume of a hyperbolic knot complement combinatorially from the knot diagram in many cases. Although we need Yokota's assumptions 1–6 and the existence of an essential solution, this method can be useful for many cases. Especially, the diagrams of 2-bridge knots in [13] satisfy Yokota's assumptions, and the existence of an essential solution of Thurston

[1] When Yokota defined his potential function, he considered the formal substitution up to sign. This consideration can effect the definition of the optimistic limit up to modulo $2\pi^2$. Therefore, although Theorem 1.1.2 holds modulo $4\pi^2$, we consider the formal substitution up to sign and the optimistic limit up to modulo $2\pi^2$.

triangulation was explained in Section 4 of [1]. Therefore, we can obtain the complex volumes of 2-bridge knots combinatorially by picking up the unique representation which gives the maximal volume.

This article consists of the following contents. In Section 2, we describe Yokota triangulation and Thurston triangulation, which corresponds to the Kashaev invariant and the colored Jones invariant respectively. We show that these two triangulations are related by 3-2 moves and 4-5 moves on some crossings. In Section 3, the potential functions V and W are defined. Especially, W is defined by the formal substitution of the colored Jones invariant. In Section 4, we prove $\mathcal{H}_2 = \left\{\exp\left(w_l \frac{\partial W}{\partial w_l}\right) = 1 \mid l = 1, \ldots, m\right\}$ is the hyperbolicity equations. In Section 5, we introduce dilogarithm identities and then complete the proof using these identities.

2 Two ideal triangulations of the knot complement

In this section, we explain two ideal triangulations of the knot complement. One is Yokota triangulation corresponding to the Kashaev invariant in [19] and the other is Thurston triangulation corresponding to the colored Jones invariant in [14]. A good reference of this section is [10], which contains wonderful pictures.

2.1 Yokota triangulation

Consider a hyperbolic knot K and its diagram D. (See Figure 1(a).) We define *sides* of D as arcs connecting two adjacent crossing points. For example, Figure 1(a) has 16 edges.

Now split a side of D open so as to make a (1,1)-tangle diagram and label crossings with integers. (See Figure 1(b).) Yokota assumed several conditions on the (1,1)-tangle diagram. (For the exact statements, see Assumptions 1–6 in [19].) The assumptions roughly mean that we remove all the crossing points that can be reduced trivially. Also, let the two open sides be I and J. Assume I and J are in an over-bridge and in an under-bridge respectively. Now extend I and J so that non-boundary endpoints of I and J become the first under-crossing point and the last over-crossing point respectively, as in Figure 1(b). Then assume the two non-boundary endpoints of I and J do not coincide. Yokota proved in [19] that we can always choose I and J with these conditions because, if not, then the knot should be the trefoil knot, which is not hyperbolic.

To obtain an ideal triangulation, place an ideal octahedron $\mathrm{A}_n\mathrm{B}_n\mathrm{C}_n\mathrm{D}_n\mathrm{E}_n\mathrm{F}_n$ on each crossing n as in Figure 2(a). We call the edges $\mathrm{A}_n\mathrm{B}_n$, $\mathrm{B}_n\mathrm{C}_n$, $\mathrm{C}_n\mathrm{D}_n$ and $\mathrm{D}_n\mathrm{A}_n$ of the octahedron *horizontal edges*. Figure 2(b) shows the positions of A_n, B_n, C_n, D_n and the horizontal edges. We twist the octahedron by identifying edges $\mathrm{A}_n\mathrm{E}_n$ to $\mathrm{C}_n\mathrm{E}_n$ and $\mathrm{B}_n\mathrm{F}_n$ to $\mathrm{D}_n\mathrm{F}_n$ as in Figure 2(a). (The actual shape of the result was appeared in [10].) Then we glue the faces of the twisted octahedron following the knot diagram. For example, in Figure 2(b), we glue $\triangle\mathrm{A}_1\mathrm{D}_1\mathrm{F}_1 \cup \triangle\mathrm{A}_1\mathrm{B}_1\mathrm{F}_1$ to $\triangle\mathrm{C}_2\mathrm{D}_2\mathrm{F}_2 \cup \triangle\mathrm{C}_2\mathrm{B}_2\mathrm{F}_2$, $\triangle\mathrm{A}_2\mathrm{D}_2\mathrm{F}_2 \cup \triangle\mathrm{A}_2\mathrm{B}_2\mathrm{F}_2$ to $\triangle\mathrm{A}_3\mathrm{D}_3\mathrm{E}_3 \cup \triangle\mathrm{C}_3\mathrm{D}_3\mathrm{E}_3$, $\triangle\mathrm{A}_3\mathrm{B}_3\mathrm{E}_3 \cup \triangle\mathrm{C}_3\mathrm{B}_3\mathrm{E}_3$ to $\triangle\mathrm{A}_4\mathrm{D}_4\mathrm{E}_4 \cup \triangle\mathrm{C}_4\mathrm{D}_4\mathrm{E}_4$, $\triangle\mathrm{A}_4\mathrm{B}_4\mathrm{E}_4 \cup \triangle\mathrm{C}_4\mathrm{B}_4\mathrm{E}_4$ to $\triangle\mathrm{C}_5\mathrm{D}_5\mathrm{F}_5 \cup \triangle\mathrm{C}_5\mathrm{B}_5\mathrm{F}_5$, and so on. Finally, we glue $\triangle\mathrm{A}_5\mathrm{B}_5\mathrm{E}_5 \cup \triangle\mathrm{C}_5\mathrm{B}_5\mathrm{E}_5$ to $\triangle\mathrm{C}_1\mathrm{D}_1\mathrm{F}_1 \cup$

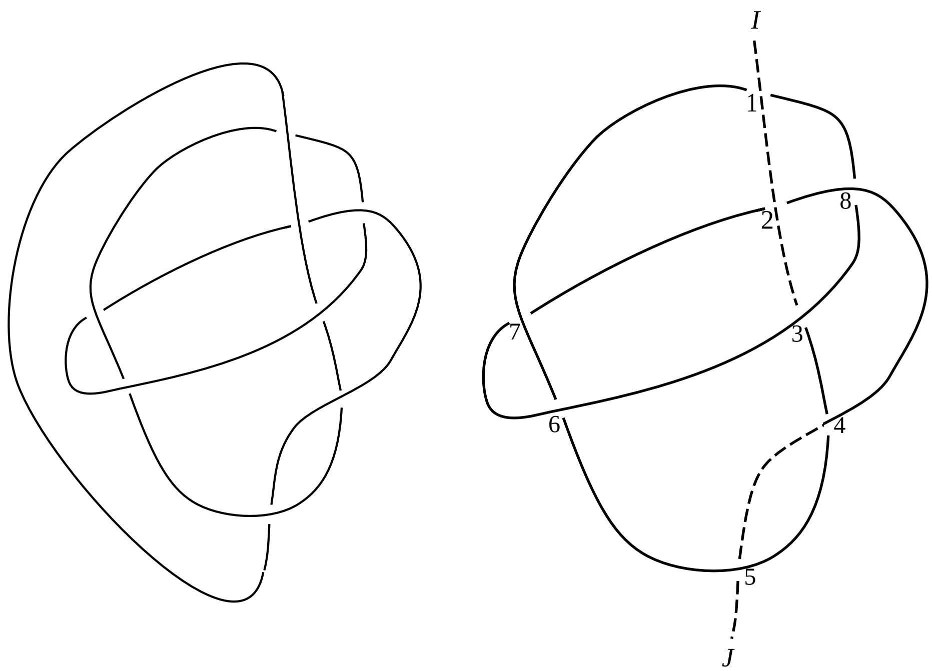

(a) Knot (b) (1,1)-tangle

Figure 1: Example

$\triangle C_1B_1F_1$. Note that, by this gluing, all A_n and C_n are identified to a point, all B_n and D_n are identified to another point, and all E_n and F_n are identified to another point. Let these points be $-\infty$, ∞ and ℓ respectively. Then the regular neighborhoods of $-\infty$ and ∞ become 3-balls, whereas the one of ℓ becomes the tubular neighborhood of the knot K.

Note that each octahedron $A_nB_nC_nD_nE_nF_n$ can be split into four tetrahedra, $A_nB_nE_nF_n$, $B_nC_nE_nF_n$, $C_nD_nE_nF_n$ and $D_nA_nE_nF_n$. If we split the octahedron in this way, then the gluing process of the ideal tetrahedra becomes the same one with Weeks triangulation in [18]. To deform the gluing result into the ideal triangualtion of the knot complement, Weeks added tunnels connecting the balls and the tubular neighborhood. However, in our case, Yokota used different method by collapsing some faces and edges of the octahedra to obtain the same result.[2]

We collapse faces that lies on the split sides. For example, in Figure 2(b), we collapse the faces $\triangle A_5B_5E_5 \cup \triangle C_5B_5E_5$ and $\triangle C_1D_1F_1 \cup \triangle C_1B_1F_1$ to different points. Note that this face collapsing makes some other edges on these faces be collapsed to points. Actually the edges B_2F_2, D_2F_2, D_3E_3, A_4F_4, and A_8B_8, B_4C_4, A_6B_6, A_7B_7 in Figure 2(b) are collapsed to points because of the face collapsing. This makes the tetrahedra $A_1B_1E_1F_1$, $B_1C_1E_1F_1$, $C_1D_1E_1F_1$, $D_1A_1E_1F_1$, $A_2B_2E_2F_2$, $B_2C_2E_2F_2$, $C_2D_2E_2F_2$, $D_2A_2E_2F_2$, $C_3D_3E_3F_3$, $D_3A_3E_3F_3$, $D_4A_4E_4F_1$, $A_4B_4E_4F_4$, $A_5B_5E_5F_5$, $B_5C_5E_5F_5$, $C_5D_5E_5F_5$, $D_5A_5E_5F_5$ and $A_8B_8E_8F_8$, $B_4C_4E_4F_4$, $A_6B_6E_6F_6$, $A_7B_7E_7F_7$ be collapsed to points or edges.

[2] We learned this difference from Yoshiyuki Yokota and Jiyoung Ham.

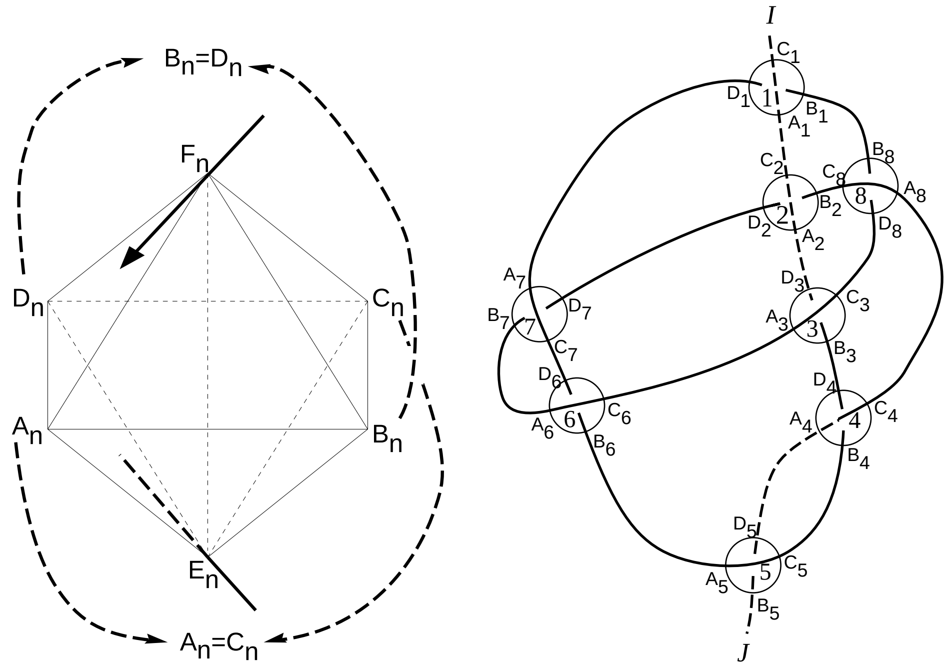

(a) Octahedron on the crossing n (b) Octahedra on corssings

Figure 2: Example(continued)

The survived tetrahedra after the collapsing can be depicted as follows. At first, remove I and J on the tangle diagram and denote the result G. (See Figure 3.) Note that, by removing $I \cup J$, some vertices are removed, two vertices become trivalent and some sides are glued together. In the example, vertices 1, 2, 5 are removed, 3, 5 become trivalent and G has 9 sides. (We consider the trivalent vertices do not glue any sides.) Now we remove the circle on the removed vertices, the arcs of the circle that is adjacent to $I \cup J$ and the arcs in the unbounded region. (See Figure 3 for the result.) The survived arcs mean the survived ideal tetrahedra after the collapsing. In the example, 12 survived tetrahedra are survived.

The collapsing identifies the points ∞, $-\infty$, ℓ each other and connects the regular neighborhoods of them. Collapsing certain edges of a tetrahedron may change the topological type of ℓ, but Yokota excluded such cases by Assumptions 1–3 on the shape of the knot diagram. Therefore, the result of the collapsing makes the neighborhood of $\infty = -\infty = \ell$ to be the tubular neighborhood of the knot, and we obtain the ideal triangulation of the knot complement. (See [19] for a complete discussion.)

2.2 Thurston triangulation

Thurston triangulation, introduced in [14], uses the same octahedra and the same collapsing process, so it also induces an ideal triangulation of the knot complement. However it uses different subdivision of each octahedra. In Figure 2(a), Yokota triangulation subdivides each

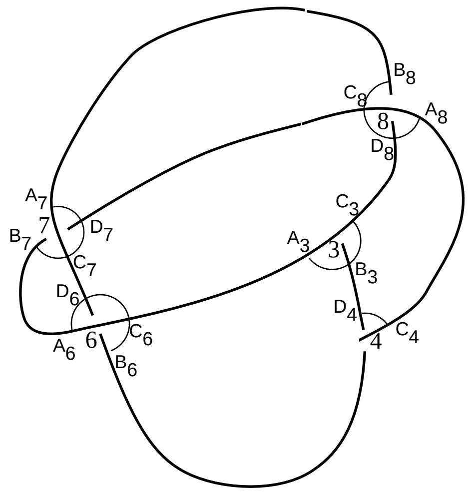

Figure 3: G with survived tetrahedra

octahedron into four tetrahedra. However, Thurston triangulation subdivides it into five tetrahedra, $A_nB_nC_nF_n$, $A_nD_nC_nF_n$, $A_nB_nC_nD_n$, $A_nB_nD_nE_n$ and $C_nB_nD_nE_n$. (See the right side of Figure 4(a) for the shape of the subdivision.)

To see the relation of these two triangulations, we define *4-5 move* of an octahedron and *3-2 move* of a hexahedron as in Figure 4.

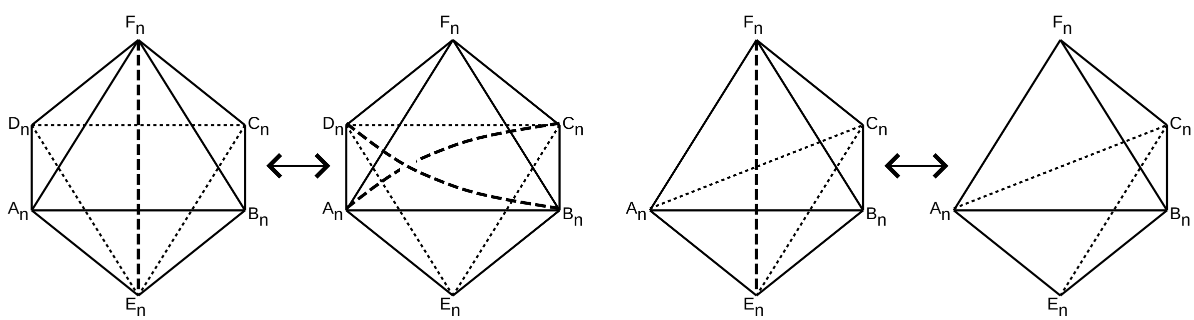

(a) 4-5 move (b) 3-2 move

Figure 4: 4-5 and 3-2 moves

Before the collapsing process, two triangulations are related by only 4-5 moves on each crossings. However, the following observation shows they are actually related by 4-5 moves and 3-2 moves after the collapsing.

Observation 2.1 *For a hyperbolic knot K with a fixed diagram, if the diagram satisfies Yokota's Assumptions in [19], then the Yokota triangulation and Thurston triangulation are related by 3-2 moves and 4-5 moves on some crossings.*

Proof. At first, for a vertex n of G, we show only one horizontal edge in Figure 2(a) can be collapsed. If any of two edges are collapsed, then the tangle diagram should be Figure 5(a) or Figure 5(b) for some tangle diagrams K_1 and K_2. However, Figure 5(a) is excluded because K is a prime knot. We can also exclude Figure 5(b) because it violates Yokota's Assumption 1. Actually, in the later case, we can reduce the number of crossings as in Figure 5(b).

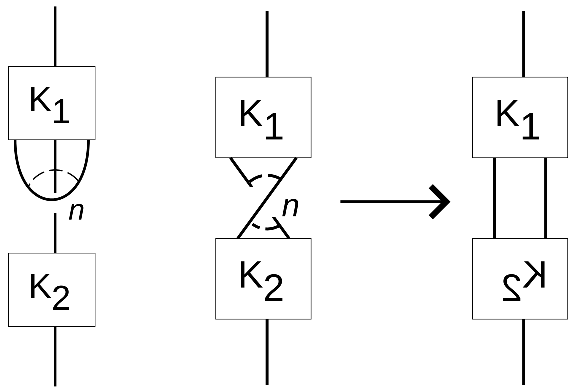

(a) (b)

Figure 5: When two horizontal edges are collapsed

Because of this and Yokota's Assumptions, all the cases of collapsing edges in Figure 5(b) are as follows :

(Case 1) if n is a non-trivalent vertex of G, then none or one of the horizontal edges is collapsed.

(Case 2) if n is a trivalent vertex of G, then

1. $\mathrm{D}_n\mathrm{E}_n$ is collapsed and none or one of $\mathrm{A}_n\mathrm{B}_n$, $\mathrm{B}_n\mathrm{C}_n$ is collapsed,
2. $\mathrm{B}_n\mathrm{E}_n$ is collapsed and none or one of $\mathrm{C}_n\mathrm{D}_n$, $\mathrm{D}_n\mathrm{A}_n$ is collapsed,
3. $\mathrm{A}_n\mathrm{F}_n$ is collapsed and none or one of $\mathrm{B}_n\mathrm{C}_n$, $\mathrm{C}_n\mathrm{D}_n$ is collapsed.

It is trivial in (Case 1), so we consider the first case of (Case 2).

If $\mathrm{D}_n\mathrm{E}_n$ and $\mathrm{A}_n\mathrm{B}_n$ are collapsed, then the survived tetrahedron is $\mathrm{B}_n\mathrm{C}_n\mathrm{E}_n\mathrm{F}_n$ in Yokota triangulation, and $\mathrm{B}_n\mathrm{C}_n\mathrm{D}_n\mathrm{F}_n$ in Thurston triangulation. They coincide because $\mathrm{D}_n = \mathrm{E}_n$ by the collapsing of $\mathrm{D}_n\mathrm{E}_n$.

If $\mathrm{D}_n\mathrm{E}_n$ is collpased and no others, then the survived tetrahedra are $\mathrm{A}_n\mathrm{B}_n\mathrm{E}_n\mathrm{F}_n$ and $\mathrm{B}_n\mathrm{C}_n\mathrm{E}_n\mathrm{F}_n$ in Yokota triangulation, and $\mathrm{A}_n\mathrm{B}_n\mathrm{D}_n\mathrm{F}_n$, $\mathrm{B}_n\mathrm{C}_n\mathrm{D}_n\mathrm{F}_n$, $\mathrm{A}_n\mathrm{B}_n\mathrm{C}_n\mathrm{D}_n$ and $\mathrm{A}_n\mathrm{B}_n\mathrm{C}_n\mathrm{E}_n$ in Thurston triangulation. However, in Thurston triangulation, two tetrahedra $\mathrm{A}_n\mathrm{B}_n\mathrm{C}_n\mathrm{D}_n$ and $\mathrm{A}_n\mathrm{B}_n\mathrm{C}_n\mathrm{E}_n$ are canceled each other because they share the same vertices A_n, B_n ,C_n and $\mathrm{D}_n = \mathrm{E}_n$. The others coincide with the tetrahedra in Yokota triangulation because $\mathrm{D}_n = \mathrm{E}_n$.

Other cases of (Case 2) is the same with the first case, so the proof is completed.

□

3 Potential functions

3.1 The case of Kashaev invariant

In the case of Kashaev invariant, Yokota's potential function can be expressed by the following simple way.

For the graph G, we define *contributing sides* as sides of G which are not on the unbounded regions. For example, there are 5 contributing sides and 4 non-contributing sides in Figure 3. We assign complex variables $z_1, \ldots, z_g$ to contributing sides and real number 1 to non-contributing sides. Now we label each ideal tetrahedra with $IT_1, IT_2, \ldots, IT_s$ and assign t_l ($l = 1, \ldots, s$) as the complex parameter of IT_l. We define t_l as the counterclockwise ratio of the two adjacent sides of IT_l.

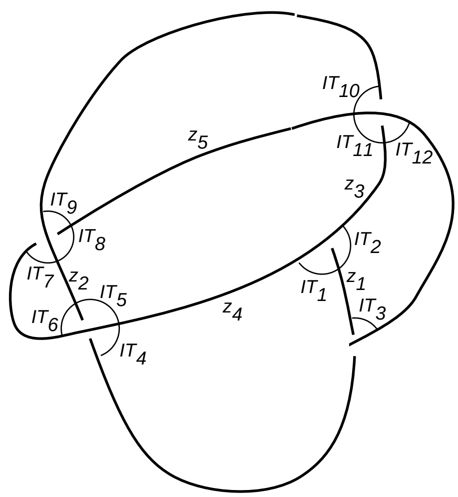

Figure 6: G with contributing sides

For example, in Figure 6,

$$t_1 = \frac{z_1}{z_4},\ t_2 = \frac{z_3}{z_1},\ t_3 = \frac{z_1}{1},\ t_4 = \frac{z_4}{1},\ t_5 = \frac{z_2}{z_4},\ t_6 = \frac{1}{z_2},$$

$$t_7 = \frac{z_2}{1},\ t_8 = \frac{z_5}{z_2},\ t_9 = \frac{1}{z_5},\ t_{10} = \frac{z_5}{1},\ t_{11} = \frac{z_3}{z_5},\ t_{12} = \frac{1}{z_3}.$$

For each tetrahedron IT_l, we assign dilogarithm function as in Figure 7. Then we define $V(z_1, \ldots, z_g)$ by the summation of all these dilogarithm functions. We also define the sign σ_l of IT_l by

$$\sigma_l = \begin{cases} 1 & \text{if } IT_l \text{ lies as in Figure 7(a)}, \\ -1 & \text{if } IT_l \text{ lies as in Figure 7(b)}. \end{cases}$$

Then $V(z_1, \ldots, z_g)$ is expressed by

$$V(z_1, \ldots, z_g) = \sum_{l=1}^{g} \sigma_l \left(\mathrm{Li}_2(t_l^{\sigma_l}) - \frac{\pi^2}{6} \right).$$

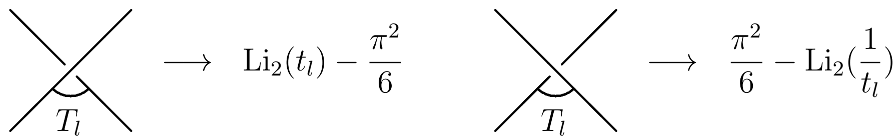

(a) Positive crossing (b) Negative crossing

Figure 7: Assignning dilogarithm functions to each tetrahedra

For example, in Figure 6,

$$\sigma_1 = \sigma_3 = \sigma_5 = \sigma_8 = \sigma_{11} = 1, \ \sigma_2 = \sigma_4 = \sigma_6 = \sigma_7 = \sigma_9 = \sigma_{10} = \sigma_{12} = -1,$$

and

$$\begin{aligned} V(z_1, \ldots, z_5) = &\mathrm{Li}_2(\frac{z_1}{z_4}) - \mathrm{Li}_2(\frac{z_1}{z_3}) + \mathrm{Li}_2(z_1) - \mathrm{Li}_2(\frac{1}{z_4}) + \mathrm{Li}_2(\frac{z_2}{z_4}) - \mathrm{Li}_2(z_2) \\ &-\mathrm{Li}_2(\frac{1}{z_2}) + \mathrm{Li}_2(\frac{z_5}{z_2}) - \mathrm{Li}_2(z_5) - \mathrm{Li}_2(\frac{1}{z_5}) + \mathrm{Li}_2(\frac{z_3}{z_5}) - \mathrm{Li}_2(z_3) + \frac{\pi^2}{3}. \end{aligned}$$

It was shown in [20] that $V(z_1, \ldots, z_g)$ can be obtained by the formal substitution of the Kashaev invariant.

3.2 The case of colored Jones invariant

Before introducing the formal substitution of the colored Jones invariant, note that the colored Jones invariant is determined by the local maxima, the local minima and the R-matrix. (See [8] for a reference.) However, as seen in (1), the local maxima and the local minima does not have an effect on the formal substitution. So we consider the R-matrix only. The R-matrix we are using is the one in [8].

In this case, we consider G with an orientation. We assign 0 to one bounded region of G, and then assign variables $r_1, \ldots, r_m$ to the other bounded regions of G and r_{m+1} to the unbounded region. Then assign variables to each sides according to the sum of variables of adjacent regions with orientations. (See Figure 8 for an example.)

For each non-trivalent vertex of G, we apply the formal substitution (1) to each R-matrix and substitute q^{r_n} to w_n as below. In the substitution process, if $r_n = 0$ then we put $w_n = 1$.[3] Note that we apply the same R-matrix in different forms according to the position of the collapsed horizontal edge. If none of the horizontal edges is collapsed in the octahedron, then we choose any formal substitution among the four possibilities. We will show in Lemma 3.1 that this choice does not change the optimistic limit .

[3] While applying the formal substitution, we ignored the term $q^{\pm N^2/4}$ in all R-matrices because this term disappears when we calculate the colored Jones invariant using the enhanced Yang-Baxter equation in [17]. This can be easily proved from the fact that $(R_J, \delta_{j,k} q^{(2j+1-N)/2}, q^{(N^2-1)/4}, 1)$ satisfies the enhanced Yang-Baxter equation by LEMMA 4.5. of [11], where R_J is the R-matrix we are using. On the other hand, we also ignore the sign of the R-matrix for the reason explained in Section 1.

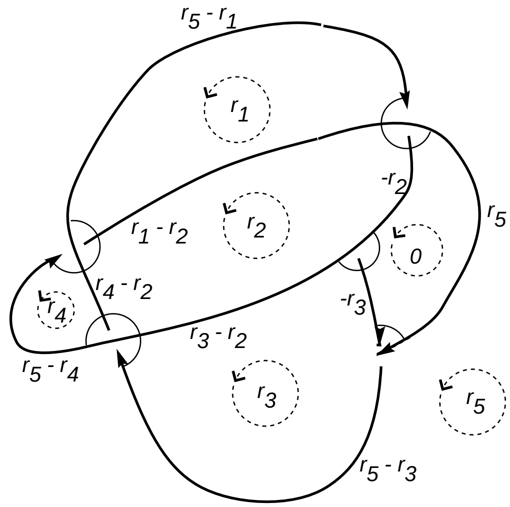

Figure 8: Assigning variables on each regions and sides

For positive crossings :

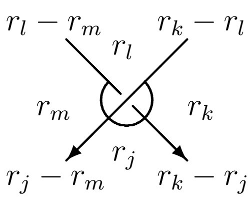

$$: \frac{(q)^{-1}_{r_l-r_m}(q^{-1})_{r_k-r_l}}{(q^{-1})_{r_k+r_m-r_j-r_l}(q^{-1})_{r_j-r_m}(q)^{-1}_{r_k-r_j}}(-1)^{r_l+r_j+1} \times q^{-(r_m-r_j)(r_k-r_j)+(r_l+r_j-2r_m)/2+(N^2+1)/4}$$

$$\sim \exp\left\{\frac{N}{2\pi i}\left(\mathrm{Li}_2(\frac{w_l}{w_m}) + \mathrm{Li}_2(\frac{w_l}{w_k}) - \mathrm{Li}_2(\frac{w_j w_l}{w_k w_m}) - \mathrm{Li}_2(\frac{w_m}{w_j}) - \mathrm{Li}_2(\frac{w_k}{w_j}) + \frac{\pi^2}{6} - \log\frac{w_m}{w_j}\log\frac{w_k}{w_j}\right)\right\},$$

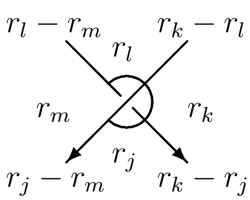

$$: \frac{(q^{-1})^{-1}_{r_l-r_m}(q^{-1})_{r_k-r_l}}{(q)_{r_k+r_m-r_j-r_l}(q^{-1})_{r_j-r_m}(q^{-1})^{-1}_{r_k-r_j}}(-1)^{r_l+r_j+1} \times q^{(r_k-r_l)(r_k-r_j)+(2r_k-r_l-r_j)/2+(N^2+1)/4}$$

$$\sim \exp\left\{\frac{N}{2\pi i}\left(-\mathrm{Li}_2(\frac{w_m}{w_l}) + \mathrm{Li}_2(\frac{w_l}{w_k}) + \mathrm{Li}_2(\frac{w_k w_m}{w_j w_l}) - \mathrm{Li}_2(\frac{w_m}{w_j}) + \mathrm{Li}_2(\frac{w_j}{w_k}) - \frac{\pi^2}{6} + \log\frac{w_k}{w_l}\log\frac{w_k}{w_j}\right)\right\},$$

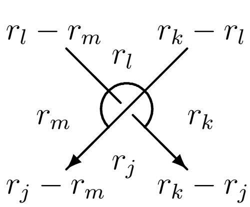

$$: \frac{(q^{-1})^{-1}_{r_l-r_m}(q)_{r_k-r_l}}{(q^{-1})_{r_k+r_m-r_j-r_l}(q)_{r_j-r_m}(q^{-1})^{-1}_{r_k-r_j}}(-1)^{r_l+r_j+1} \times q^{-(r_m-r_l)(r_k-r_l)+(r_l+r_j-2r_m)/2+(N^2+1)/4}$$

$$\sim \exp\left\{\frac{N}{2\pi i}\left(-\mathrm{Li}_2(\frac{w_m}{w_l}) - \mathrm{Li}_2(\frac{w_k}{w_l}) - \mathrm{Li}_2(\frac{w_j w_l}{w_k w_m}) + \mathrm{Li}_2(\frac{w_j}{w_m}) + \mathrm{Li}_2(\frac{w_j}{w_k}) + \frac{\pi^2}{6} - \log\frac{w_m}{w_l}\log\frac{w_k}{w_l}\right)\right\},$$

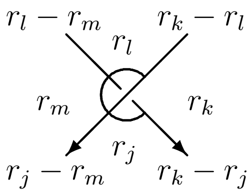

$$: \frac{(q)^{-1}_{r_l-r_m}(q)_{r_k-r_l}}{(q)_{r_k+r_m-r_j-r_l}(q)_{r_j-r_m}(q)^{-1}_{r_k-r_j}}(-1)^{r_l+r_j+1} \times q^{(r_m-r_l)(r_m-r_j)+(r_l+r_j-2r_m)/2+(N^2+1)/4}$$

$$\sim \exp\left\{\frac{N}{2\pi i}\left(\mathrm{Li}_2(\tfrac{w_l}{w_m})-\mathrm{Li}_2(\tfrac{w_k}{w_l})+\mathrm{Li}_2(\tfrac{w_kw_m}{w_jw_l})+\mathrm{Li}_2(\tfrac{w_j}{w_m})-\mathrm{Li}_2(\tfrac{w_k}{w_j})-\tfrac{\pi^2}{6}+\log\tfrac{w_m}{w_l}\log\tfrac{w_m}{w_j}\right)\right\}.$$

For negative crossings :

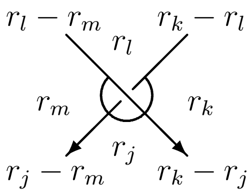

$$: \frac{(q)_{r_l-r_m}(q^{-1})^{-1}_{r_k-r_l}}{(q)_{r_j+r_l-r_k-r_m}(q^{-1})^{-1}_{r_j-r_m}(q)_{r_k-r_j}}(-1)^{r_l+r_j+1} \times q^{(r_j-r_m)(r_j-r_k)-(2r_k-r_l-r_j)/2-(N^2+1)/4}$$

$$\sim \exp\left\{\frac{N}{2\pi i}\left(-\mathrm{Li}_2(\tfrac{w_l}{w_m})-\mathrm{Li}_2(\tfrac{w_l}{w_k})+\mathrm{Li}_2(\tfrac{w_jw_l}{w_kw_m})+\mathrm{Li}_2(\tfrac{w_m}{w_j})+\mathrm{Li}_2(\tfrac{w_k}{w_j})-\tfrac{\pi^2}{6}+\log\tfrac{w_j}{w_m}\log\tfrac{w_j}{w_k}\right)\right\},$$

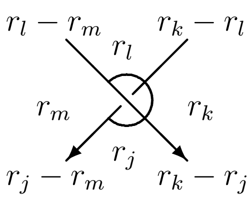

$$: \frac{(q^{-1})_{r_l-r_m}(q^{-1})^{-1}_{r_k-r_l}}{(q^{-1})_{r_j+r_l-r_k-r_m}(q^{-1})^{-1}_{r_j-r_m}(q^{-1})_{r_k-r_j}}(-1)^{r_l+r_j+1} \times q^{-(r_l-r_k)(r_j-r_k)-(2r_k-r_l-r_j)/2-(N^2+1)/4}$$

$$\sim \exp\left\{\frac{N}{2\pi i}\left(\mathrm{Li}_2(\tfrac{w_m}{w_l})-\mathrm{Li}_2(\tfrac{w_l}{w_k})-\mathrm{Li}_2(\tfrac{w_kw_m}{w_jw_l})+\mathrm{Li}_2(\tfrac{w_m}{w_j})-\mathrm{Li}_2(\tfrac{w_j}{w_k})+\tfrac{\pi^2}{6}-\log\tfrac{w_l}{w_k}\log\tfrac{w_j}{w_k}\right)\right\},$$

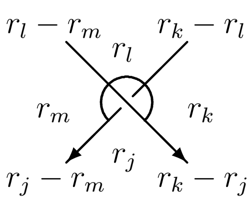

$$: \frac{(q^{-1})_{r_l-r_m}(q)^{-1}_{r_k-r_l}}{(q)_{r_j+r_l-r_k-r_m}(q)^{-1}_{r_j-r_m}(q^{-1})_{r_k-r_j}}(-1)^{r_l+r_j+1} \times q^{(r_l-r_m)(r_l-r_k)-(2r_k-r_l-r_j)/2-(N^2+1)/4}$$

$$\sim \exp\left\{\frac{N}{2\pi i}\left(\mathrm{Li}_2(\tfrac{w_m}{w_l})+\mathrm{Li}_2(\tfrac{w_k}{w_l})+\mathrm{Li}_2(\tfrac{w_jw_l}{w_kw_m})-\mathrm{Li}_2(\tfrac{w_j}{w_m})-\mathrm{Li}_2(\tfrac{w_j}{w_k})-\tfrac{\pi^2}{6}+\log\tfrac{w_l}{w_m}\log\tfrac{w_l}{w_k}\right)\right\},$$

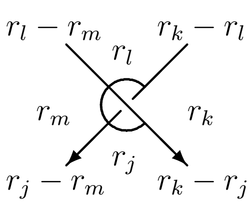

$$: \frac{(q)_{r_l-r_m}(q)^{-1}_{r_k-r_l}}{(q^{-1})_{r_j+r_l-r_k-r_m}(q)^{-1}_{r_j-r_m}(q)_{r_k-r_j}}(-1)^{r_l+r_j+1} \times q^{-(r_l-r_m)(r_j-r_m)-(r_l+r_j-2r_m)/2-(N^2+1)/4}$$

$$\sim \exp\left\{\frac{N}{2\pi i}\left(-\mathrm{Li}_2(\tfrac{w_l}{w_m})+\mathrm{Li}_2(\tfrac{w_k}{w_l})-\mathrm{Li}_2(\tfrac{w_kw_m}{w_jw_l})-\mathrm{Li}_2(\tfrac{w_j}{w_m})+\mathrm{Li}_2(\tfrac{w_k}{w_j})+\tfrac{\pi^2}{6}-\log\tfrac{w_l}{w_m}\log\tfrac{w_j}{w_m}\right)\right\}.$$

For the trivalent vertices of G, we assign 0 to the sides in I or J and then apply the same formal substitution to the R-matrix as follows. (In here, we do not concern the collapsing of the horizontal edges of the octahedron.)

For the end point of I :

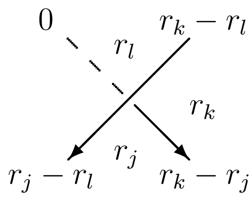

$$: \ \frac{(q)_{r_k-r_l}}{(q)_{r_j-r_l}}(-1)^{r_l+r_j+1}q^{(r_j-r_l)/2+(N^2+1)/4} \sim \exp\left\{\frac{N}{2\pi i}\left(-\mathrm{Li}_2(\tfrac{w_k}{w_l})+\mathrm{Li}_2(\tfrac{w_j}{w_l})\right)\right\},$$

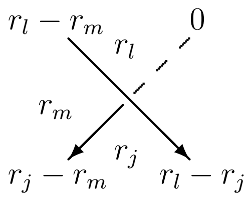

$$: \ \frac{(q^{-1})_{r_l-r_m}}{(q^{-1})_{r_l-r_j}}(-1)^{r_l+r_j+1}q^{-(r_l-r_j)/2-(N^2+1)/4} \sim \exp\left\{\frac{N}{2\pi i}\left(\mathrm{Li}_2(\tfrac{w_m}{w_l})-\mathrm{Li}_2(\tfrac{w_j}{w_l})\right)\right\}.$$

For the end point of J :

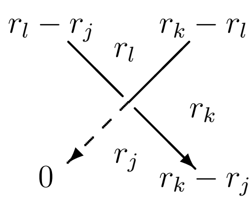

$$: \ \frac{(q)_{r_k-r_j}}{(q)_{r_l-r_j}}(-1)^{r_l+r_j+1}q^{(r_l-r_j)/2+(N^2+1)/4} \sim \exp\left\{\frac{N}{2\pi i}\left(-\mathrm{Li}_2(\tfrac{w_k}{w_j})+\mathrm{Li}_2(\tfrac{w_l}{w_j})\right)\right\},$$

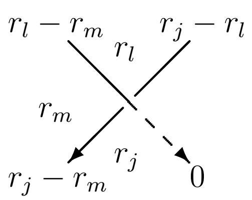

$$: \ \frac{(q^{-1})_{r_j-r_m}}{(q^{-1})_{r_j-r_l}}(-1)^{r_l+r_j+1}q^{-(r_j-r_l)/2-(N^2+1)/4} \sim \exp\left\{\frac{N}{2\pi i}\left(\mathrm{Li}_2(\tfrac{w_m}{w_j})-\mathrm{Li}_2(\tfrac{w_l}{w_j})\right)\right\}.$$

Now we define a potential function $\widetilde{W}(w_1,\ldots,w_{m+1})$ of the knot diagram by letting the product of all formal substitutions to be $\exp\left\{\frac{N}{2\pi i}\widetilde{W}(w_1,\ldots,w_{m+1})\right\}$. One important thing of $\widetilde{W}$ is that the parameter w_{m+1} assigned to the unbounded region always appears as numerator. Therefore, we can define another potential function $W(w_1,\ldots,w_m) := \widetilde{W}(w_1,\ldots,w_m,0)$.[4] Note that using W instead of $\widetilde{W}$ does not violate the definition of the optimistic limit because, for a solution $(w_1^{(0)},\ldots,w_m^{(0)})$ of $\left\{\exp\left(w_l\frac{\partial W}{\partial w_l}\right)=1 \,|\, l=1,\ldots,m\right\}$, $(w_1^{(0)},\ldots,w_m^{(0)},0)$ becomes a solution of $\left\{\exp\left(w_l\frac{\partial W}{\partial w_l}\right)=1 \,|\, l=1,\ldots,m+1\right\}$. We remark that this W is the potential function appeared in Theorem 1.1.

[4]Note that $\mathrm{Li}_2(0)=0$.

For an example, $\widetilde{W}$ and W of Figure 8 become

$$\begin{aligned}\widetilde{W}(w_1,\ldots,w_5) &= \left\{-\mathrm{Li}_2(\frac{1}{w_2})+\mathrm{Li}_2(\frac{w_3}{w_2})\right\}+\left\{-\mathrm{Li}_2(\frac{w_5}{w_3})+\mathrm{Li}_2(\frac{1}{w_3})\right\}\\
&+\left\{-\mathrm{Li}_2(\frac{w_3}{w_2})+\mathrm{Li}_2(\frac{w_5}{w_3})-\mathrm{Li}_2(\frac{w_5w_2}{w_4w_3})-\mathrm{Li}_2(\frac{w_4}{w_2})+\mathrm{Li}_2(\frac{w_5}{w_4})+\frac{\pi^2}{6}-\log\frac{w_3}{w_2}\log\frac{w_4}{w_2}\right\}\\
&+\left\{-\mathrm{Li}_2(\frac{w_4}{w_2})+\mathrm{Li}_2(\frac{w_5}{w_4})-\mathrm{Li}_2(\frac{w_5w_2}{w_1w_4})-\mathrm{Li}_2(\frac{w_1}{w_2})+\mathrm{Li}_2(\frac{w_5}{w_1})+\frac{\pi^2}{6}-\log\frac{w_4}{w_2}\log\frac{w_1}{w_2}\right\}\\
&+\left\{-\mathrm{Li}_2(\frac{w_1}{w_2})+\mathrm{Li}_2(\frac{w_5}{w_1})-\mathrm{Li}_2(\frac{w_5w_2}{w_1})-\mathrm{Li}_2(\frac{1}{w_2})+\mathrm{Li}_2(w_5)+\frac{\pi^2}{6}-\log\frac{w_1}{w_2}\log\frac{1}{w_2}\right\},\end{aligned}$$

and

$$\begin{aligned}W(w_1,\ldots,w_4) = -2\left\{\mathrm{Li}_2(\frac{1}{w_2})+\mathrm{Li}_2(\frac{w_4}{w_2})+\mathrm{Li}_2(\frac{w_1}{w_2})\right\}+\mathrm{Li}_2(\frac{1}{w_3})+\frac{\pi^2}{2}\\
-\log\frac{w_3}{w_2}\log\frac{w_4}{w_2}-\log\frac{w_4}{w_2}\log\frac{w_1}{w_2}-\log\frac{w_1}{w_2}\log\frac{1}{w_2}.\end{aligned}$$

We close this section with the discussion of the invariance of the optimistic limit under the choice of the four different forms of the R-matrix.

Lemma 3.1 *Let the four formal substitutions of the R-matrix of the positive crossing be* $\exp\left\{\frac{N}{2\pi i}P_f(w_j,w_k,w_l,w_m)\right\}$ *and the ones of the negative crossing be* $\exp\left\{\frac{N}{2\pi i}N_f(w_j,w_k,w_l,w_m)\right\}$ *for* $f=1,\ldots,4$*. Also let*

$$P_{f0}:=P_f-\sum_{a=j,k,l,m}\left(w_a\frac{\partial P_f}{\partial w_a}\right)\log w_a,\;\; N_{f0}:=N_f-\sum_{a=j,k,l,m}\left(w_a\frac{\partial N_f}{\partial w_a}\right)\log w_a.$$

Then

$$P_{10}\equiv P_{20}\equiv P_{30}\equiv P_{40},\;\; N_{10}\equiv N_{20}\equiv N_{30}\equiv N_{40}\pmod{4\pi^2},$$

and

$$\begin{aligned}\exp\left(w_a\frac{\partial P_1}{\partial w_a}\right)=\exp\left(w_a\frac{\partial P_2}{\partial w_a}\right)=\exp\left(w_a\frac{\partial P_3}{\partial w_a}\right)=\exp\left(w_a\frac{\partial P_4}{\partial w_a}\right),\\
\exp\left(w_a\frac{\partial N_1}{\partial w_a}\right)=\exp\left(w_a\frac{\partial N_2}{\partial w_a}\right)=\exp\left(w_a\frac{\partial N_3}{\partial w_a}\right)=\exp\left(w_a\frac{\partial N_4}{\partial w_a}\right).\end{aligned}$$

Proof. For a given complex valued function $F(w_j,w_k,w_l,w_m)$, let

$$F_0(w_j,w_k,w_l,w_m):=F-\sum_{a=j,k,l,m}\left(w_a\frac{\partial F}{\partial w_a}\right)\log w_a,$$

and

$$\widehat{F}(w_j,w_k,w_l,w_m):=F+\sum_{a=j,k,l,m}2n_a\pi i\log w_a+4n\pi^2, \tag{3}$$

for some integer constants n_j, n_k, n_l, n_m, n. Then, by the direct calculation,

$$\widehat{F}_0 \equiv F_0 \pmod{4\pi^2},$$

and

$$\exp\left(w_a \frac{\partial F}{\partial w_a}\right) = \exp\left(w_a \frac{\partial \widehat{F}}{\partial w_a}\right).$$

Therefore, we define an equivalence relation $\approx$ by $F \approx \widehat{F}$ for F and $\widehat{F}$ satisfying (3).

For

$$\begin{aligned}
P_1 &= \mathrm{Li}_2(\frac{w_l}{w_m}) + \mathrm{Li}_2(\frac{w_l}{w_k}) - \mathrm{Li}_2(\frac{w_j w_l}{w_k w_m}) - \mathrm{Li}_2(\frac{w_m}{w_j}) - \mathrm{Li}_2(\frac{w_k}{w_j}) + \frac{\pi^2}{6} - \log\frac{w_m}{w_j}\log\frac{w_k}{w_j}, \\
P_2 &= -\mathrm{Li}_2(\frac{w_m}{w_l}) + \mathrm{Li}_2(\frac{w_l}{w_k}) + \mathrm{Li}_2(\frac{w_k w_m}{w_j w_l}) - \mathrm{Li}_2(\frac{w_m}{w_j}) + \mathrm{Li}_2(\frac{w_j}{w_k}) - \frac{\pi^2}{6} + \log\frac{w_k}{w_l}\log\frac{w_k}{w_j},
\end{aligned}$$

using the well-known identity $\mathrm{Li}_2(z) + \mathrm{Li}_2(\frac{1}{z}) = -\frac{\pi^2}{6} - \frac{1}{2}\log^2(-z)$ for $z \in \mathbb{C}$ in [6], we obtain

$$\begin{aligned}
P_1 - P_2 &= \mathrm{Li}_2(\frac{w_l}{w_m}) + \mathrm{Li}_2(\frac{w_m}{w_l}) - \mathrm{Li}_2(\frac{w_j w_l}{w_k w_m}) - \mathrm{Li}_2(\frac{w_k w_m}{w_j w_l}) \\
&\quad - \mathrm{Li}_2(\frac{w_k}{w_j}) - \mathrm{Li}_2(\frac{w_j}{w_k}) + \frac{\pi^2}{3} - \left(\log\frac{w_m}{w_j} + \log\frac{w_k}{w_l}\right)\log\frac{w_k}{w_j} \\
&= \frac{\pi^2}{2} - \frac{1}{2}\log^2(-\frac{w_l}{w_m}) + \frac{1}{2}\log^2(-\frac{w_k w_m}{w_j w_l}) + \frac{1}{2}\log^2(-\frac{w_k}{w_j}) - \left(\log\frac{w_m}{w_j} + \log\frac{w_k}{w_l}\right)\log\frac{w_k}{w_j}.
\end{aligned}$$

Remark that, for some integers $n_1, \ldots, n_5$, we have

$$\begin{aligned}
&2n_1\pi i\log\frac{w_k}{w_j} = 2n_1\pi i\,(\log w_k - \log w_j + 2n_2\pi i) \approx 0, \\
&\frac{1}{2}\log^2(-\frac{w_k}{w_j}) = \frac{1}{2}\left\{\log\frac{w_k}{w_j} + (2n_3 - 1)\pi i\right\}^2 \\
&\quad = \frac{1}{2}\log^2\frac{w_k}{w_j} + (2n_3 - 1)\pi i\log\frac{w_k}{w_j} - 2n_3(n_3 - 1)\pi^2 - \frac{\pi^2}{2} \\
&\quad \approx \frac{1}{2}\log^2\frac{w_k}{w_j} - \pi i\log\frac{w_k}{w_j} - \frac{\pi^2}{2},
\end{aligned}$$

and

$$\begin{aligned}
&\frac{1}{2}\left\{\log\frac{w_k}{w_j} - \log(-\frac{w_k w_m}{w_j w_l})\right\}^2 = \frac{1}{2}\left\{\log(-\frac{w_l}{w_m}) + 2n_4\pi i\right\}^2 \\
&\quad = \frac{1}{2}\log^2(-\frac{w_l}{w_m}) + 2n_4\pi i\left\{\log\frac{w_l}{w_m} + (2n_5 + 1)\pi i\right\} - 2n_4^2\pi^2 \\
&\quad \approx \frac{1}{2}\log^2(-\frac{w_l}{w_m}) - 2n_4(n_4 + 1)\pi^2 \approx \frac{1}{2}\log^2(-\frac{w_l}{w_m}).
\end{aligned}$$

Therefore, we obtain

$$\begin{aligned}
&P_1 - P_2 \\
&\approx -\frac{1}{2}\log^2(-\frac{w_l}{w_m}) + \frac{1}{2}\log^2(-\frac{w_k w_m}{w_j w_l}) + \frac{1}{2}\log^2\frac{w_k}{w_j} - \pi i \log\frac{w_k}{w_j} - \log\frac{w_k w_m}{w_j w_l}\log\frac{w_k}{w_j} \\
&\approx -\frac{1}{2}\log^2(-\frac{w_l}{w_m}) + \frac{1}{2}\log^2(-\frac{w_k w_m}{w_j w_l}) + \frac{1}{2}\log^2\frac{w_k}{w_j} - \log(-\frac{w_k w_m}{w_j w_l})\log\frac{w_k}{w_j} \\
&= -\frac{1}{2}\log^2(-\frac{w_l}{w_m}) + \frac{1}{2}\left\{\log\frac{w_k}{w_j} - \log(-\frac{w_k w_m}{w_j w_l})\right\}^2 \approx -\frac{1}{2}\log^2(-\frac{w_l}{w_m}) + \frac{1}{2}\log^2(-\frac{w_l}{w_m}) = 0.
\end{aligned}$$

Other equalities $P_2 \approx P_3 \approx P_4$ and $N_1 \approx N_2 \approx N_3 \approx N_4$ can be obtained by the same method or by the symmetry of the equations. □

4 Geometric structures of the triangulations

For Yokota triangulation and Thurston triangulation, we assign complex variables on each tetrahedra and solve certain equations. Then one of the solutions gives the complete hyperbolic structure of the knot complement. We describe these procedure in this section.

At first, consider the following positive and negative crossings in Figure 9, where z_a, z_b, z_c, z_d are assigned to the edges of G from Yokota triangulation and r_j, r_k, r_l, r_m are assigned to the regions of G from Thurston triangulation.

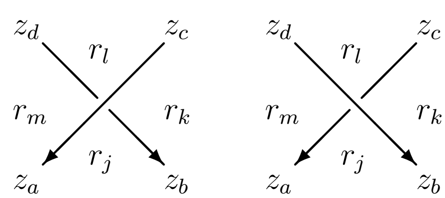

Figure 9: Assignment of variables

Then consider Figure 10. We assign $\frac{z_b}{z_a}, \frac{z_c}{z_b}, \frac{z_d}{z_c}, \frac{z_a}{z_d}$ to the horizontal edges $\mathrm{A}_n\mathrm{B}_n$, $\mathrm{B}_n\mathrm{C}_n$, $\mathrm{C}_n\mathrm{D}_n$, $\mathrm{D}_n\mathrm{A}_n$ respectively. Also, for the positive crossing, we assign $\left(\frac{w_j}{w_m}\right)^{-1}, \frac{w_k}{w_j}, \frac{w_k}{w_l}, \left(\frac{w_l}{w_m}\right)^{-1}$ to $\mathrm{A}_n\mathrm{F}_n$, $\mathrm{B}_n\mathrm{E}_n$, $\mathrm{C}_n\mathrm{F}_n$, $\mathrm{D}_n\mathrm{E}_n$ respectively, and assign $\left(\frac{w_k w_m}{w_j w_l}\right)^{-1}$ to $\mathrm{B}_n\mathrm{D}_n$ and $\mathrm{A}_n\mathrm{C}_n$ for the parameter of the tetrahedron $\mathrm{A}_n\mathrm{B}_n\mathrm{C}_n\mathrm{D}_n$. For the negative crossing, we assign $\frac{w_j}{w_m}, \left(\frac{w_k}{w_j}\right)^{-1}, \left(\frac{w_k}{w_l}\right)^{-1}, \frac{w_l}{w_m}$ to $\mathrm{D}_n\mathrm{E}_n$, $\mathrm{A}_n\mathrm{F}_n$, $\mathrm{B}_n\mathrm{D}_n$, $\mathrm{B}_n\mathrm{E}_n$, $\mathrm{C}_n\mathrm{F}_n$ respectively, and assign $\left(\frac{w_j w_l}{w_k w_m}\right)^{-1}$ to $\mathrm{B}_n\mathrm{D}_n$ and $\mathrm{A}_n\mathrm{C}_n$ for the parameter of the tetrahedron $\mathrm{A}_n\mathrm{B}_n\mathrm{C}_n\mathrm{D}_n$.

We do not assign any variables to the collapsed edges. Also, in the case of Thurston triangulation, we do not assign any variables to the edges that contain the endpoints of the collapsed edges. For example, if $\mathrm{C}_n\mathrm{D}_n$ is collapsed, then we do not assign any variables to

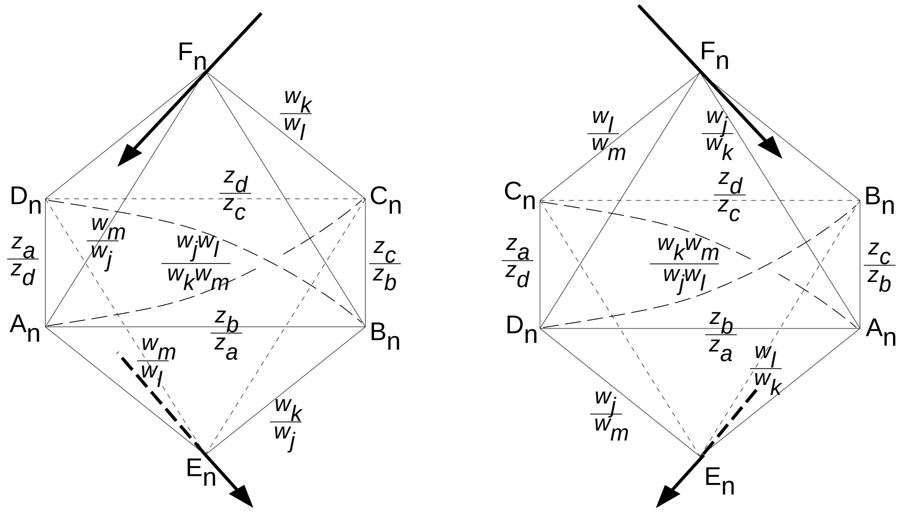

(a) Positive crossing (b) Negative crossing

Figure 10: Assignment of variables

C_nF_n, D_nE_n and B_nD_n. Also, if D_nE_n is collapsed in Figure 10(a), then we do not assign any variables to B_nD_n, B_nE_n, C_nD_n and D_nA_n.[5]

Yokota and Thurston triangulations are ideal triangulations, so by assigning these variables, we can parametrize all ideal tetrahedra of the triangulations. Note that if we assign a variable $u \in \mathbb{C}$ to an edge of an ideal tetrahedron, then the other edges are also parametrized by $u, u' := \frac{1}{1-u}$ and $u'' := 1 - \frac{1}{u}$ as in Figure 11.

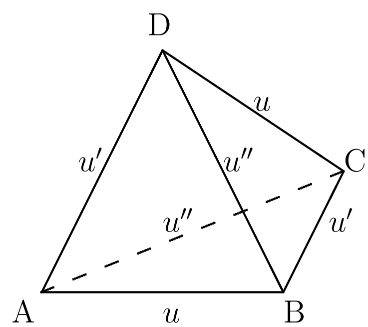

Figure 11: Parametrization of an ideal tetrahedron with a parameter u

So as to get the hyperbolic structure, these variables should satisfy the *edges relations* and the *cusp conditions*. The edge relations mean the product of all variables assigned to one edge should be one, and the cusp conditions mean the holonomies induced by the longitude and the meridian should be translations. These two conditions can be expressed by set of

[5] The edges C_nD_n and D_nA_n are horizontal edges, but are identified to non-horizontal edges. When this happens, we do not assign variables to these edges.

equations of the variables, so we call the set of equations *hyperbolicity equations*. (For details, see Chapter 4 of [15].) We call a solution $(z_1, \ldots, z_g)$ of the hyperbolicity equations of Yokota triangulation *essential* if none of the variables of the tetrahedra are one of $0, 1, \pm\infty$. We also define an *essential solution* $(w_1, \ldots, w_m)$ of Thurston triangulation in the same way. It is a well-known fact that if the hyperbolicity equations have an essential solution, then they have the unique solution which gives the hyperbolic structure to the triangulation.[6] (For details, see Section 2.8 of [16].) We call the unique solution *geometric solution*. We remark that, from Observation 2.1, the existence of the geometric solution of Yokota triangulation is equivalent to that of Thurston triangulation. We denote the geometric solution of Yokota triangulation $(z_1^{(0)}, \ldots, z_g^{(0)})$ and the one of Thurston triangulation $(w_1^{(0)}, \ldots, w_m^{(0)})$.

Yokota proved in [19] that, for the potential function V defined in Section 3.1, $\mathcal{H}_1 = \left\{\exp\left(z_k \frac{\partial V}{\partial z_k}\right) = 1 \mid k = 1, \ldots, g\right\}$ becomes the hyperbolicity equations of Yokota triangulation. In other words, each element of $\mathcal{H}_1$ becomes an edge relation or a cusp condition for all $k = 1, \ldots, g$, and all the other equations can be induced from these.

We show that the same relation holds for the potential function W defined in Section 3.2. Let $\mathcal{A}$ be the set of non-collapsed horizontal edges of the Thurston triangulation of $S^3 - K$. Let $\mathcal{B}$ be the set of non-collapsed non-horizontal edges $\mathrm{A}_n\mathrm{E}_n$, $\mathrm{B}_n\mathrm{E}_n$, $\mathrm{C}_n\mathrm{E}_n$, $\mathrm{D}_n\mathrm{E}_n$, $\mathrm{A}_n\mathrm{F}_n$, $\mathrm{B}_n\mathrm{F}_n$, $\mathrm{C}_n\mathrm{F}_n$, $\mathrm{D}_n\mathrm{F}_n$ in Figure 10, which are not in $\mathcal{A}$.[7] Finally, let $\mathcal{C}$ be the set of edges $\mathrm{A}_n\mathrm{C}_n$, $\mathrm{B}_n\mathrm{D}_n$ in Figure 10, which are not in $\mathcal{A} \cup \mathcal{B}$.

For example, in Figure 3, $\mathcal{A} = \{\, \mathrm{A}_3\mathrm{B}_3 = \mathrm{B}_6\mathrm{C}_6 = \mathrm{D}_4\mathrm{A}_4 = \mathrm{D}_4\mathrm{F}_4 = \mathrm{A}_4\mathrm{B}_4 = \mathrm{B}_4\mathrm{F}_4 = \mathrm{C}_4\mathrm{F}_4 = \mathrm{A}_8\mathrm{F}_8 = \mathrm{B}_8\mathrm{F}_8 = \mathrm{D}_8\mathrm{F}_8 = \mathrm{D}_7\mathrm{E}_7,\ \mathrm{D}_6\mathrm{A}_6 = \mathrm{B}_7\mathrm{C}_7,\ \mathrm{C}_6\mathrm{D}_6 = \mathrm{C}_7\mathrm{D}_7 = \mathrm{C}_8\mathrm{D}_8 = \mathrm{D}_3\mathrm{A}_3 = \mathrm{A}_3\mathrm{E}_3 = \mathrm{C}_3\mathrm{D}_3 = \mathrm{C}_3\mathrm{E}_3 = \mathrm{A}_4\mathrm{E}_4 = \mathrm{C}_4\mathrm{E}_4 = \mathrm{B}_4\mathrm{E}_4 = \mathrm{A}_6\mathrm{E}_6 = \mathrm{B}_6\mathrm{E}_6 = \mathrm{C}_6\mathrm{E}_6 = \mathrm{C}_7\mathrm{F}_7,\ \mathrm{D}_7\mathrm{A}_7 = \mathrm{B}_8\mathrm{C}_8,\ \mathrm{C}_4\mathrm{D}_4 = \mathrm{B}_3\mathrm{C}_3 = \mathrm{D}_8\mathrm{A}_8\}$, $\mathcal{B} = \{\, \mathrm{B}_3\mathrm{E}_3 = \mathrm{D}_4\mathrm{E}_4,\ \mathrm{D}_6\mathrm{E}_6 = \mathrm{B}_7\mathrm{F}_7 = \mathrm{D}_7\mathrm{F}_7 = \mathrm{A}_7\mathrm{F}_7 = \mathrm{A}_8\mathrm{E}_8 = \mathrm{B}_8\mathrm{E}_8 = \mathrm{C}_8\mathrm{E}_8 = \mathrm{C}_3\mathrm{F}_3,\ \mathrm{A}_3\mathrm{F}_3 = \mathrm{C}_6\mathrm{F}_6,\ \mathrm{D}_8\mathrm{E}_8 = \mathrm{B}_3\mathrm{F}_3 = \mathrm{D}_3\mathrm{F}_3 = \mathrm{A}_6\mathrm{F}_6 = \mathrm{B}_6\mathrm{F}_6 = \mathrm{D}_6\mathrm{F}_6 = \mathrm{B}_7\mathrm{E}_7 = \mathrm{C}_7\mathrm{E}_7 = \mathrm{A}_7\mathrm{E}_7 = \mathrm{C}_8\mathrm{F}_8 \,\}$ and $\mathcal{C} = \emptyset$.

Lemma 4.1 *For a hyperbolic knot K with a fixed diagram, we assume all the assumptions of Theorem 1.1. Then the edges in $\mathcal{B} \cup \mathcal{C}$ satisfy the edge relations trivially by the method of parametrizing edges.*

Proof. If an edge $\mathrm{A}_n\mathrm{C}_n$ or $\mathrm{B}_n\mathrm{D}_n$ of Figure 10 is in $\mathcal{C}$, then the octahedron $\mathrm{A}_n\mathrm{B}_n\mathrm{C}_n\mathrm{D}_n\mathrm{E}_n\mathrm{F}_n$ does not have any collapsed edge. By the method of parametrizing edges, all the edges in $\mathcal{C}$ satisfy edge relations trivially.

Now we show the case of $\mathcal{B}$. Consider the following four cases of two points n and $n+1$ in Figure 12. (For the positions of the points $\mathrm{A}_n, \mathrm{B}_n, \ldots, \mathrm{F}_{n+1}$, see Figure 2.) At first, we assume no edges are collapsed in the tetrahedra between the two crossing points n and $n+1$.

In the case of Figure 12(a), we draw a part of the cusp diagram in $\mathrm{A}_n\mathrm{B}_n\mathrm{D}_n\mathrm{F}_n \cup \mathrm{B}_{n+1}\mathrm{C}_{n+1}\mathrm{D}_{n+1}\mathrm{F}_{n+1}$ near $\mathrm{F}_n = \mathrm{F}_{n+1}$ as in Figure 13. Our tetrahedra are all ideal, so the triangles $\triangle\alpha_1\alpha_2\alpha_3$ and $\triangle\alpha_1\alpha_4\alpha_5$ are Euclidean. Note that $\alpha_1, \ldots, \alpha_5$ are points in the edges $\mathrm{A}_n\mathrm{F}_n = \mathrm{C}_{n+1}\mathrm{F}_{n+1}$,

[6] Strictly speaking, we have the unique values of parameters of the ideal tetrahedra. However, these parameters uniquely determine the solutions $(z_1^{(0)}, \ldots, z_g^{(0)})$ and $(w_1^{(0)}, \ldots, w_m^{(0)})$. It was explained in [19] for Yokota triangulation, and it will be in the end of this Section for Thurston triangulation.

[7] Collapsing identify some horizontal edges to non-horizontal edges.

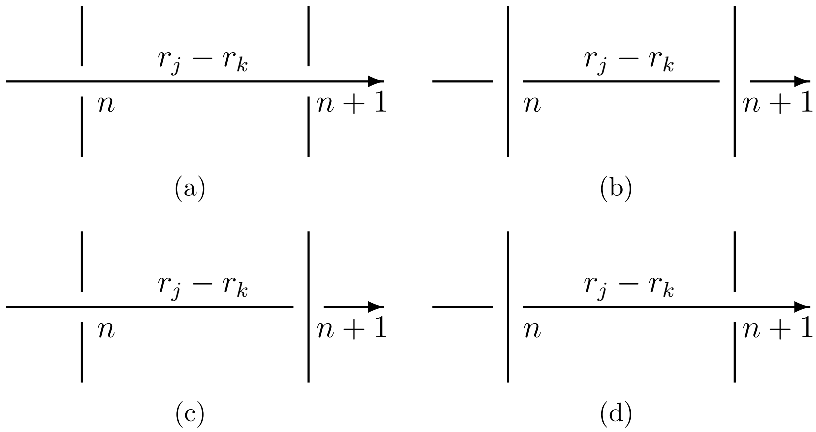

Figure 12: Four cases

$\mathrm{B}_n\mathrm{F}_n$, $\mathrm{D}_n\mathrm{F}_n$, $\mathrm{D}_{n+1}\mathrm{F}_{n+1}$, $\mathrm{B}_{n+1}\mathrm{F}_{n+1}$ respectively. Furthermore, edges $\alpha_1\alpha_2$ and $\alpha_1\alpha_3$ are identified to $\alpha_1\alpha_5$ and $\alpha_1\alpha_4$ respectively.[8] On the edge $\mathrm{A}_n\mathrm{F}_n = \mathrm{C}_{n+1}\mathrm{F}_{n+1}$, two variables w_k/w_j and w_j/w_k are assigned respectively by the assigning rule, so the edge relation of $\mathrm{A}_n\mathrm{F}_n = \mathrm{C}_{n+1}\mathrm{F}_{n+1} \in \mathcal{B}$ holds trivially.

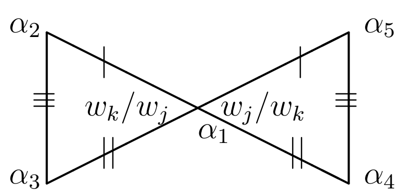

Figure 13: Part of the cusp diagram of Figure 12(a)

In the case of Figure 12(c), if $n+1$ is a positive crossing, we draw a part of the cusp diagram in $\mathrm{A}_n\mathrm{B}_n\mathrm{D}_n\mathrm{F}_n \cup \mathrm{A}_{n+1}\mathrm{C}_{n+1}\mathrm{D}_{n+1}\mathrm{E}_{n+1}$ near $\mathrm{F}_n = \mathrm{E}_{n+1}$, and if $n+1$ is a negative crossing, we draw a part of the cusp diagram in $\mathrm{A}_n\mathrm{B}_n\mathrm{D}_n\mathrm{F}_n \cup \mathrm{A}_{n+1}\mathrm{B}_{n+1}\mathrm{C}_{n+1}\mathrm{E}_{n+1}$ near $\mathrm{F}_n = \mathrm{E}_{n+1}$ as in Figure 14.

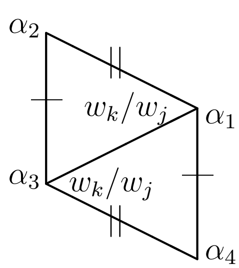

Figure 14: Part of the cusp diagram of Figure 12(c)

Note that if $n+1$ is a positive crossing, then $\alpha_1, \ldots, \alpha_4$ are points in the edges $\mathrm{A}_n\mathrm{F}_n =$

[8]In fact, edges $\alpha_2\alpha_3$ and $\alpha_5\alpha_4$ are also identified, so the two triangles are cancelled each other. This means the corresponding tetrahedra are also cancelled each other.

$A_{n+1}E_{n+1}$, B_nF_n, $D_nF_n = D_{n+1}E_{n+1}$, $C_{n+1}E_{n+1}$ respectively, and if $n+1$ is a negative crossing, then $\alpha_1, \ldots, \alpha_4$ are points in the edges $A_nF_n = C_{n+1}E_{n+1}$, B_nF_n, $D_nF_n = B_{n+1}E_{n+1}$, $A_{n+1}E_{n+1}$ respectively. Furthermore, the edge $\alpha_2\alpha_1$ is identified to $\alpha_3\alpha_4$, so the diagram in Figure 14 becomes an annulus. The product of variables around $\alpha_1 = \alpha_4$ is $\dfrac{w_k}{w_j}\left(\dfrac{w_k}{w_j}\right)'\left(\dfrac{w_k}{w_j}\right)'' = -1$, and the one around $\alpha_2 = \alpha_3$ is also -1. Therefore, if we assume $A_nF_n \in \mathcal{B}$ and consider the next annulus on the right of Figure 14, we obtain the edge relation of A_nF_n. Note that the next annulus always exists because, if not, then $A_nF_n \in \mathcal{A}$.

The cases of Figure 12(b) and Figure 12(d) are the same with the cases of Figure 12(a) and Figure 12(c) respectively. Therefore, we find all the edges in $\mathcal{B}$ satisfy the edge relations trivially by the method of parametrizing edges.

Now we assume one of the regions parametrized by r_j or r_k in Figure 12 is unbounded region. Then the cusp diagram in Figure 13 collapsed to an edge $\alpha_2\alpha_3 = \alpha_5\alpha_4$ and the one in Figure 14 collapsed to an edge $\alpha_2\alpha_3 = \alpha_1\alpha_4$. Therefore, our arguments for $\mathcal{B}$ still hold for the collapsed case.[9]

□

Lemma 4.2 *For a hyperbolic knot K with a fixed diagram, we assume all the assumptions of Theorem 1.1. Let* $\mathcal{H}_2 = \left\{\exp\left(w_l \frac{\partial W}{\partial w_l}\right) = 1 \mid l = 1, \ldots, m\right\}$ *for the potential function W defined in Section 3.2. Then $\mathcal{H}_2$ gives all the edge relations of $\mathcal{C}$.*

Proof. Consider the function $P_1(w_j, w_k, w_l, w_m)$, which are defined in Lemma 3.1. By direct calculation, we obtain

$$\exp\left(w_j \frac{\partial P_1}{\partial w_j}\right) = \left\{\left(\frac{w_j w_l}{w_k w_m}\right)'\left(\frac{w_m}{w_j}\right)''\left(\frac{w_k}{w_j}\right)''\right\}^{-1}, \tag{4}$$

$$\exp\left(w_k \frac{\partial P_1}{\partial w_k}\right) = \left\{\left(\frac{w_j w_l}{w_k w_m}\right)''\left(\frac{w_k}{w_l}\right)'\left(\frac{w_k}{w_j}\right)'\right\}^{-1}, \tag{5}$$

$$\exp\left(w_l \frac{\partial P_1}{\partial w_l}\right) = \left\{\left(\frac{w_j w_l}{w_k w_m}\right)'\left(\frac{w_m}{w_l}\right)''\left(\frac{w_k}{w_l}\right)''\right\}^{-1}, \tag{6}$$

$$\exp\left(w_m \frac{\partial P_1}{\partial w_m}\right) = \left\{\left(\frac{w_j w_l}{w_k w_m}\right)''\left(\frac{w_m}{w_l}\right)'\left(\frac{w_m}{w_j}\right)'\right\}^{-1}. \tag{7}$$

Note that the reciprocals of (4), (5), (6) and (7) are the product of variables assigned to the edges A_nB_n, B_nC_n, C_nD_n and D_nA_n of Figure 10(a) respectively. Also, after evaluating

[9] We remark that the product of variables on $\alpha_3 = \alpha_4$ in Figure 12 is $\left(\frac{w_k}{w_j}\right)''\left(\frac{w_j}{w_k}\right)' = 1$, and the one on $\alpha_2 = \alpha_5$ is also 1. Therefore, even if α_1 is identified to $\alpha_3 = \alpha_4$ or $\alpha_2 = \alpha_5$ in Figure 12, the edge relation of α_1 is trivially satisfied.

$w_l = 0$ to P_1, we obtain

$$\exp\left(w_j \frac{\partial P_1(w_j, w_k, 0, w_m)}{\partial w_j}\right) = \left\{\left(\frac{w_m}{w_j}\right)'' \left(\frac{w_k}{w_j}\right)''\right\}^{-1}, \tag{8}$$

$$\exp\left(w_k \frac{\partial P_1(w_j, w_k, 0, w_m)}{\partial w_k}\right) = \left\{\frac{w_m}{w_j} \left(\frac{w_k}{w_j}\right)'\right\}^{-1}, \tag{9}$$

$$\exp\left(w_m \frac{\partial P_1(w_j, w_k, 0, w_m)}{\partial w_m}\right) = \left\{\left(\frac{w_m}{w_j}\right)' \frac{w_k}{w_j}\right\}^{-1}. \tag{10}$$

Note that the reciprocals of (8), (9) and (10) are the product of variables assigned to the edges $\mathrm{A}_n\mathrm{B}_n$, $\mathrm{B}_n\mathrm{C}_n$ and $\mathrm{D}_n\mathrm{A}_n$ of Figure 10(a) respectively after collapsing the edge $\mathrm{C}_n\mathrm{D}_n$. Direct calculation shows the same relations hold for P_2, P_3, P_4, N_1, N_2, N_3 and N_4.

Let the two formal substitutions of the R-matrices for the end point of I in Section 3.2 be $\exp\left\{\frac{N}{2\pi i} I_1(w_j, w_k, w_l)\right\}$ and $\exp\left\{\frac{N}{2\pi i} I_2(w_j, w_l, w_m)\right\}$ respectively, and the ones for the end point of J be $\exp\left\{\frac{N}{2\pi i} J_1(w_j, w_k, w_l)\right\}$ and $\exp\left\{\frac{N}{2\pi i} J_2(w_j, w_l, w_m)\right\}$ respectively. Direct calculation shows

$$\exp\left(w_k \frac{\partial I_1(w_j, w_k, w_l)}{\partial w_k}\right) = \exp\left(w_k \frac{\partial I_1(0, w_k, w_l)}{\partial w_k}\right) = \left\{\left(\frac{w_k}{w_l}\right)'\right\}^{-1}, \tag{11}$$

$$\exp\left(w_j \frac{\partial I_1(w_j, w_k, w_l)}{\partial w_j}\right) = \exp\left(w_j \frac{\partial I_1(w_j, 0, w_l)}{\partial w_j}\right) = \left\{\left(\frac{w_l}{w_j}\right)''\right\}^{-1}, \tag{12}$$

$$\exp\left(w_l \frac{\partial I_1(w_j, w_k, w_l)}{\partial w_l}\right) = \left\{\left(\frac{w_j}{w_l}\right)' \left(\frac{w_l}{w_k}\right)''\right\}^{-1} = \left\{\left(\frac{w_l}{w_j}\right)' \left(\frac{w_k}{w_l}\right)'' \frac{w_k}{w_j}\right\}^{-1}, \tag{13}$$

$$\exp\left(w_l \frac{\partial I_1(0, w_k, w_l)}{\partial w_l}\right) = \left\{\left(\frac{w_l}{w_k}\right)''\right\}^{-1} = \left\{\left(\frac{w_k}{w_l}\right)'' \frac{w_k}{w_l} (-1)\right\}^{-1}, \tag{14}$$

$$\exp\left(w_l \frac{\partial I_1(w_j, 0, w_l)}{\partial w_l}\right) = \left\{\left(\frac{w_j}{w_l}\right)'\right\}^{-1} = \left\{\left(\frac{w_l}{w_j}\right)' \frac{w_l}{w_j} (-1)\right\}^{-1}, \tag{15}$$

where (11) and (12) are the reciprocals of the product of variables assigned to the edges $\mathrm{B}_n\mathrm{C}_n$ and $\mathrm{A}_n\mathrm{B}_n$ of Figure 10(a) after collapsing the edge $\mathrm{D}_n\mathrm{E}_n$ respectively without or with the collapsing of a horizontal edge.[10]

To explain that the reciprocals of (13), (14) and (15) are still a part of an edge relation, we need more discussion. At first, see Figure 13 and Figure 14 again as in Figure 15.

In Figure 15(a), the product of all variables assigned to the dot is

$$\left(\frac{w_a}{w_b}\right)' \left(\frac{w_a}{w_b}\right)'' \left(\frac{w_b}{w_a}\right)' \left(\frac{w_b}{w_a}\right)'' = 1, \tag{16}$$

and in Figure 15(b), the product is

$$\left(\frac{w_a}{w_b}\right)' \left(\frac{w_a}{w_b}\right)'' \frac{w_a}{w_b} = -1. \tag{17}$$

[10]We denote $r_m := r_l$ and $w_m := w_l$ in this case.

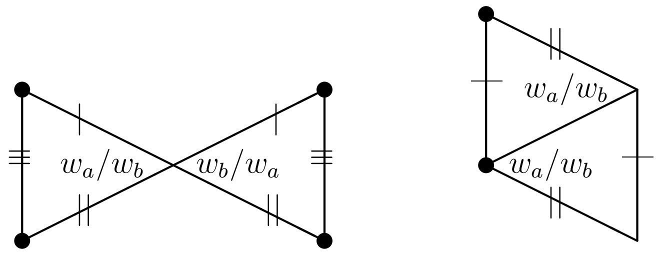

(a) From Figure 13 (b) From Figure 14

Figure 15: Parts of the cusp diagram from Figure 13 and Figure 14

To see the meaning of (13), consider the following two cases in Figure 16, where n is the end point of I and $n+1$ is the next over-crossing point.

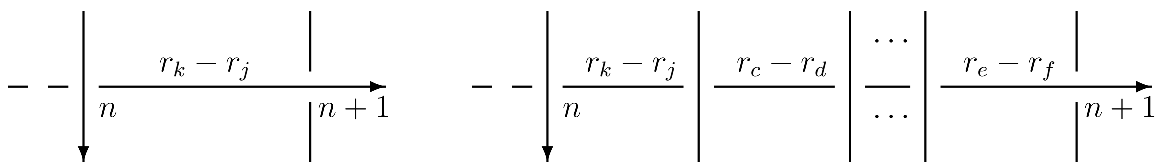

(a) (b)

Figure 16: Two cases after the end point of I

The parts of the cusp diagram of each cases are as in Figure 17.

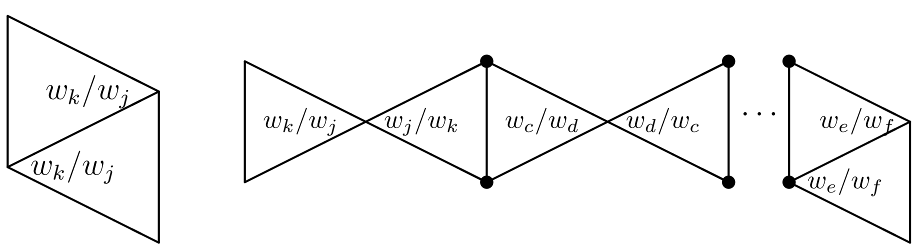

(a) (b)

Figure 17: The parts of the cusp diagram corresponding to Figure 16

In the case of Figure 16(a), the product of variables assigned to the edges $\mathrm{C}_n\mathrm{D}_n = \mathrm{D}_n\mathrm{A}_n$ of Figure 10(a) is $\left(\frac{w_l}{w_j}\right)'\left(\frac{w_k}{w_l}\right)''$. These edges are identified to $\mathrm{C}_{n+1}\mathrm{F}_{n+1}$, and $\frac{w_k}{w_j}$ is assigned to this edge. This explains the reciprocals of (13) is the product of variables assigned to the edges $\mathrm{C}_n\mathrm{D}_n = \mathrm{D}_n\mathrm{A}_n = \mathrm{C}_{n+1}\mathrm{F}_{n+1}$.

In the case of Figure 16(b), the product of variables assigned to the edges $\mathrm{C}_n\mathrm{D}_n = \mathrm{D}_n\mathrm{A}_n$ of Figure 10(a) is $\left(\frac{w_l}{w_j}\right)'\left(\frac{w_k}{w_l}\right)''$. In Figure 17(b), these edges are identified to the edges represented by the dots, and the product of variables assigned to the dots is

$$\left(\frac{w_j}{w_k}\right)'\left(\frac{w_j}{w_k}\right)'' \times 1 \times \cdots \times (-1) = \frac{w_k}{w_j}$$

by (16) and (17). This also explains the reciprocals of (13) is the product of variables assigned to $\mathrm{C}_n\mathrm{D}_n = \mathrm{D}_n\mathrm{A}_n$ and some others identified to this. This fact is still true[11] when some of the regions assigned by $r_c, \ldots, r_f$ are unbounded regions because the collapsing of the horizontal edges makes the cusp diagrams of Figure 13 and Figure 14 edges. If the cusp diagram of Figure 13 becomes an edge, then removing it is enough for our consideration, and if that of Figure 14 becomes an edge, then consider the next annulus is enough. The next annulus always exists because, if not, the knot diagram violates Yokota's Assumption 5 in [19].

Now we describe the meaning of (14). Let n be the end point of I, $n+1$ be the next over-crossing point and $n+2$ be the next under-crossing point. Also let $\tilde{n}$ be the next point of n. Assume the edges $\mathrm{D}_n\mathrm{E}_n$ and $\mathrm{A}_n\mathrm{B}_n$ of Figure 10(a) are collapsed. Then $\mathrm{C}_n\mathrm{D}_n = \mathrm{B}_n\mathrm{D}_n$ and $\left(\frac{w_k}{w_l}\right)'' \frac{w_k}{w_l}$ is assigned to this edge. If $n = \tilde{n}$, then the edges identified to $\mathrm{C}_n\mathrm{D}_n = \mathrm{B}_n\mathrm{D}_n$ are appeared between the points $n+1$ and $n+2$ as the dots in Figure 15, and if $n \neq \tilde{n}$, then the edges are appeared between $\tilde{n}$ and $n+1$ as the same way. Especially, Figure 15(a) may appear many times, but Figure 15(b) appears only one time at the point $n+2$ or $n+1$ respectively. By (16) and (17), the product of all variables assigned to the dots is -1, so the reciprocal of (14) is the product of variables assigned to the edges $\mathrm{C}_n\mathrm{D}_n = \mathrm{B}_n\mathrm{D}_n$ and some others identified to these. This fact is still true when some of the horizontal edges or non-horizontal edges of the octahedra are collapsed because of the same reason explained in the case of (13) above.

The same relations hold for (15) and the case of I_2, J_1, J_2 by the similar arguments.

Therefore, we conclude that $\mathcal{H}_2$ becomes all the edge relations of $\mathcal{A}$ except the one horizontal edge whose region is assigned with 0 instead of the variables $r_1, \ldots, r_m$. For an ideal tetrahedron parametrized with $u \in \mathbb{C}$ as in Figure 11, the product of all variables assigned to all edges in the tetrahedron is $(uu'u'')^2 = 1$. This implies all the product of all edge relations becomes 1. On the other hand, from Lemma 4.1 and the above arguments, we found all the edge relations become 1 by assuming $\mathcal{H}_2$ except one edge relation. Therefore, the edge relation of the left edge holds automatically and the proof is done.

□

Note that $\alpha_1\alpha_4$ and $\alpha_3\alpha_2$ in Figure 14 are meridians of the cusp diagram. The same variable $\frac{w_k}{w_j}$ is assigned to the corners $\angle\alpha_2\alpha_1\alpha_3$ and $\angle\alpha_1\alpha_3\alpha_4$, so one of the cusp condition is trivially satisfied by the method of parametrizing edges. If we have all the edge relations and one cusp condition of a meridian, then we can obtain all the other cusp conditions using these relations. Therefore, by Lemma 4.1 and Lemma 4.2, we conclude $\mathcal{H}_2$ is the hyperbolicity equations of Thurston triangulation of $S^3 - K$.

We remark a technical fact. For Thurston triangulation, let the parameters of the ideal tetrahedra be $s_1, \ldots, s_h$. These parameters are defined by the ratios of a solution $w_1, \ldots, w_m$ of $\mathcal{H}_2$, so if the values of $w_1, \ldots, w_m$ are fixed, then the values of $s_1, \ldots, s_h$ are uniquely determined trivially and satisfy the hyperbolicity equation. Likewise, if the values of $s_1, \ldots, s_h$ satisfying the hyperbolicity equations are fixed, then we can uniquely determine the solution of $w_1, \ldots, w_m$ of $\mathcal{H}_2$ as follows: At first, we can determine some of the values of $w_1, \ldots, w_m$,

[11] Even if the endpoint of J is between the crossings n and $n+1$, this fact is still true because the collapsing of the non-horizontal edges does not change the part of the cusp diagram we are considering.

which are assigned to the regions adjacent to the region assigned with the number 0. Once a value w_l of a region is determined, then all the values of the adjacent regions can be determined. Therefore, all $w_1, \ldots, w_m$ can be determined. Furthermore, those values are well-defined and become a solution of $\mathcal{H}_2$ because of the hyperbolicity equations.

Note that we already have a one-to-one correspondence between $(t_1, \ldots, t_g)$ of Yokota triangulation and $(s_1, \ldots, s_h)$ of Thurston triangulation by Observation 2.1. Yokota explained the one-to-one correspondence between $(t_1, \ldots, t_g)$ and $(z_1, \ldots, z_g)$ in [19], and the above explains the one-to-one correspondence between $(s_1, \ldots, s_h)$ and $(w_1, \ldots, w_m)$. Therefore, we obtain the one-to-one correspondence between the essential solutions of $\mathcal{H}_1$ and $\mathcal{H}_2$. This correspondence is the one used in Theorem 1.1 and Corollary 1.2 to find the solution w of $\mathcal{H}_2$ corresponding to a solution z of $\mathcal{H}_1$, and vice versa.

5 Proof of Main Theorem

We already proved the first part of Theorem 1.1 in Section 4 and the existence of $(w_1, \ldots, w_m)$ and $(w_1^{(0)}, \ldots, w_m^{(0)})$ corresponding to $(z_1, \ldots, z_g)$ and $(z_1^{(0)}, \ldots, z_g^{(0)})$ respectively in Observation 2.1 and Section 4. Also we defined the potential function W by the formal substitution of the colored Jones invariant in Section 3.2, so $W_0(w_1^{(0)}, \ldots, w_m^{(0)})$ becomes the optimistic limit. Therefore it is enough to show

$$V_0(z_1, \ldots, z_g) \equiv -W_0(w_1, \ldots, w_m) \pmod{4\pi^2},$$

for any essential solution $(z_1, \ldots, z_g)$ of $\mathcal{H}_1$ and the corresponding essential solution $(w_1, \ldots, w_m)$ of $\mathcal{H}_2$. To prove it, we introduce dilogarithm identities of an ideal octahedron. We assign variables t_1, t_2, t_3, t_4, u_1, u_2, u_3 and u_4 to the edges AB, BC, CD, DA, AF, BE, CF and DE respectively at the ideal octahedron in Figure 18. Let $u_5 := \frac{1}{u_1 u_3} = \frac{1}{u_2 u_4}$.

Then we obtain the following relations.

$$\begin{cases} u_1 = t_1' t_4'', \\ u_2 = t_1' t_2'', \\ u_3 = t_3' t_2'', \\ u_4 = t_3' t_4'', \\ u_5 = (t_1' t_2'' t_3' t_4'')^{-1}, \end{cases} \qquad \begin{cases} t_1 = u_1'' u_2'' u_5', \\ t_2 = u_2' u_3' u_5'', \\ t_3 = u_3'' u_4'' u_5', \\ t_4 = u_4' u_1' u_5'', \\ t_1 t_2 t_3 t_4 = 1. \end{cases} \tag{18}$$

Let $D(z) := \operatorname{Im} \operatorname{Li}_2(z) + \log|z| \arg(1-z)$ be the Bloch-Wigner function for $z \in \mathbb{C} - \{0, 1\}$. It is a well-known fact that $D(z) = \operatorname{vol}(T_z)$ where T_z is the hyperbolic ideal tetrahedron parametrized by z. Therefore, from Figure 18, we obtain

$$D(t_1) + D(t_2) + D(t_3) + D(t_4) = D(u_1) + D(u_2) + D(u_3) + D(u_4) + D(u_5). \tag{19}$$

Lemma 5.1 *Let $t_1, t_2, t_3, t_4, u_1, u_2, u_3, u_4, u_5$ be the complex variables defined in the octahedron in Figure 18, which are satisfying (18) and (19). Then the following identities hold.*

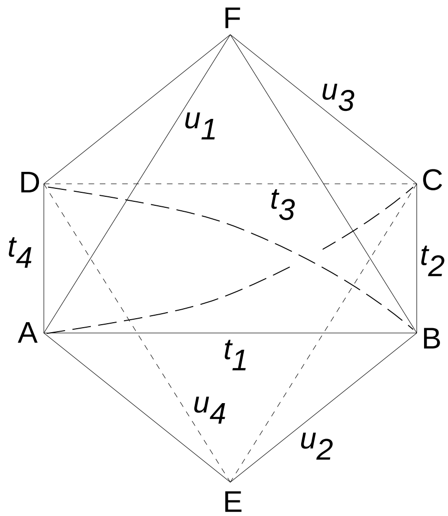

Figure 18: Assignment of variables

$$
\begin{aligned}
&\mathrm{Li}_2(t_1) - \mathrm{Li}_2(\frac{1}{t_2}) + \mathrm{Li}_2(t_3) - \mathrm{Li}_2(\frac{1}{t_4}) \\
&\quad = \mathrm{Li}_2(u_1) + \mathrm{Li}_2(u_2) - \mathrm{Li}_2(\frac{1}{u_3}) - \mathrm{Li}_2(\frac{1}{u_4}) + \mathrm{Li}_2(u_5) - \frac{\pi^2}{6} + \log u_1 \log u_2 \qquad (20)\\
&\qquad - \left(-\log(1-t_1) + \log(1-\frac{1}{t_4})\right)\log u_2 - \left(-\log(1-t_1) + \log(1-\frac{1}{t_2})\right)\log u_1 \\
&\qquad + \left(-\log(1-t_1) + \log(1-\frac{1}{t_4})\right)\log(1-u_1) + \left(-\log(1-t_1) + \log(1-\frac{1}{t_2})\right)\log(1-u_2) \\
&\qquad + \left(-\log(1-t_3) + \log(1-\frac{1}{t_2})\right)\log(1-\frac{1}{u_3}) + \left(-\log(1-t_3) + \log(1-\frac{1}{t_4})\right)\log(1-\frac{1}{u_4}) \\
&\qquad + \left(\log(1-t_1) - \log(1-\frac{1}{t_2}) + \log(1-t_3) - \log(1-\frac{1}{t_4})\right)\log(1-u_5)
\end{aligned}
$$

$$
\begin{aligned}
&\quad = \mathrm{Li}_2(u_1) - \mathrm{Li}_2(\frac{1}{u_2}) - \mathrm{Li}_2(\frac{1}{u_3}) + \mathrm{Li}_2(u_4) - \mathrm{Li}_2(\frac{1}{u_5}) + \frac{\pi^2}{6} - \log u_2 \log u_3 \qquad (21)\\
&\qquad + \left(-\log(1-t_3) + \log(1-\frac{1}{t_2})\right)\log u_2 + \left(-\log(1-t_1) + \log(1-\frac{1}{t_2})\right)\log u_3 \\
&\qquad + \left(-\log(1-t_1) + \log(1-\frac{1}{t_4})\right)\log(1-u_1) + \left(-\log(1-t_1) + \log(1-\frac{1}{t_2})\right)\log(1-\frac{1}{u_2}) \\
&\qquad + \left(-\log(1-t_3) + \log(1-\frac{1}{t_2})\right)\log(1-\frac{1}{u_3}) + \left(-\log(1-t_3) + \log(1-\frac{1}{t_4})\right)\log(1-u_4) \\
&\qquad + \left(\log(1-t_1) - \log(1-\frac{1}{t_2}) + \log(1-t_3) - \log(1-\frac{1}{t_4})\right)\log(1-\frac{1}{u_5})
\end{aligned}
$$

$$
\begin{aligned}
&= -\mathrm{Li}_2(\frac{1}{u_1}) - \mathrm{Li}_2(\frac{1}{u_2}) + \mathrm{Li}_2(u_3) + \mathrm{Li}_2(u_4) + \mathrm{Li}_2(u_5) - \frac{\pi^2}{6} + \log u_3 \log u_4 \\
&\quad - \left(-\log(1-t_3) + \log(1-\frac{1}{t_4})\right)\log u_3 - \left(-\log(1-t_3) + \log(1-\frac{1}{t_2})\right)\log u_4 \\
&\quad + \left(-\log(1-t_1) + \log(1-\frac{1}{t_4})\right)\log(1-\frac{1}{u_1}) + \left(-\log(1-t_1) + \log(1-\frac{1}{t_2})\right)\log(1-\frac{1}{u_2}) \\
&\quad + \left(-\log(1-t_3) + \log(1-\frac{1}{t_2})\right)\log(1-u_3) + \left(-\log(1-t_3) + \log(1-\frac{1}{t_4})\right)\log(1-u_4) \\
&\quad + \left(\log(1-t_1) - \log(1-\frac{1}{t_2}) + \log(1-t_3) - \log(1-\frac{1}{t_4})\right)\log(1-u_5)
\end{aligned} \tag{22}
$$

$$
\begin{aligned}
&= -\mathrm{Li}_2(\frac{1}{u_1}) + \mathrm{Li}_2(u_2) + \mathrm{Li}_2(u_3) - \mathrm{Li}_2(\frac{1}{u_4}) - \mathrm{Li}_2(\frac{1}{u_5}) + \frac{\pi^2}{6} - \log u_1 \log u_4 \\
&\quad + \left(-\log(1-t_1) + \log(1-\frac{1}{t_4})\right)\log u_4 + \left(-\log(1-t_3) + \log(1-\frac{1}{t_4})\right)\log u_1 \\
&\quad + \left(-\log(1-t_1) + \log(1-\frac{1}{t_4})\right)\log(1-\frac{1}{u_1}) + \left(-\log(1-t_1) + \log(1-\frac{1}{t_2})\right)\log(1-u_2) \\
&\quad + \left(-\log(1-t_3) + \log(1-\frac{1}{t_2})\right)\log(1-u_3) + \left(-\log(1-t_3) + \log(1-\frac{1}{t_4})\right)\log(1-\frac{1}{u_4}) \\
&\quad + \left(\log(1-t_1) - \log(1-\frac{1}{t_2}) + \log(1-t_3) - \log(1-\frac{1}{t_4})\right)\log(1-\frac{1}{u_5}).
\end{aligned} \tag{23}
$$

Furthermore,

$$
\begin{aligned}
\mathrm{Li}_2(t_1) - \mathrm{Li}_2(\frac{1}{t_2}) - \mathrm{Li}_2(\frac{1}{t_4}) + \frac{\pi^2}{6} &= \mathrm{Li}_2(u_1) + \mathrm{Li}_2(u_2) - \frac{\pi^2}{6} + \log u_1 \log u_2 \\
&\quad + \left(-\log(1-t_1) + \log(1-\frac{1}{t_4})\right)(-\log u_2 + \log(1-u_1)) \\
&\quad + \left(-\log(1-t_1) + \log(1-\frac{1}{t_2})\right)(-\log u_1 + \log(1-u_2))
\end{aligned} \tag{24}
$$

when CD is collapsed to a point,

$$
\begin{aligned}
\mathrm{Li}_2(t_1) - \mathrm{Li}_2(\frac{1}{t_2}) + \mathrm{Li}_2(t_3) - \frac{\pi^2}{6} &= -\mathrm{Li}_2(\frac{1}{u_2}) - \mathrm{Li}_2(\frac{1}{u_3}) + \frac{\pi^2}{6} - \log u_2 \log u_3 \\
&\quad + \left(-\log(1-t_3) + \log(1-\frac{1}{t_2})\right)\left(\log u_2 + \log(1-\frac{1}{u_3})\right) \\
&\quad + \left(-\log(1-t_1) + \log(1-\frac{1}{t_2})\right)\left(\log u_3 + \log(1-\frac{1}{u_2})\right)
\end{aligned} \tag{25}
$$

when DA is collapsed to a point,

$$
\begin{aligned}
-\mathrm{Li}_2(\frac{1}{t_2}) + \mathrm{Li}_2(t_3) - \mathrm{Li}_2(\frac{1}{t_4}) + \frac{\pi^2}{6} &= \mathrm{Li}_2(u_3) + \mathrm{Li}_2(u_4) - \frac{\pi^2}{6} + \log u_3 \log u_4 \\
&+ \left(-\log(1-t_3) + \log(1-\frac{1}{t_4})\right)(-\log u_3 + \log(1-u_4)) \\
&+ \left(-\log(1-t_3) + \log(1-\frac{1}{t_2})\right)(-\log u_4 + \log(1-u_3))
\end{aligned} \tag{26}
$$

when AB is collapsed to a point, and

$$
\begin{aligned}
\mathrm{Li}_2(t_1) + \mathrm{Li}_2(t_3) - \mathrm{Li}_2(\frac{1}{t_4}) - \frac{\pi^2}{6} &= -\mathrm{Li}_2(\frac{1}{u_1}) - \mathrm{Li}_2(\frac{1}{u_4}) + \frac{\pi^2}{6} - \log u_1 \log u_4 \\
&+ \left(-\log(1-t_1) + \log(1-\frac{1}{t_4})\right)\left(\log u_4 + \log(1-\frac{1}{u_1})\right) \\
&+ \left(-\log(1-t_3) + \log(1-\frac{1}{t_4})\right)\left(\log u_1 + \log(1-\frac{1}{u_4})\right)
\end{aligned} \tag{27}
$$

when BC is collapsed to a point.

Proof. After the direct calculation of the imaginary parts of (20), (21), (22), (23), they coincide with

$$
\begin{aligned}
D(t_1) - D(\frac{1}{t_2}) + D(t_3) - D(\frac{1}{t_4}) &= D(u_1) + D(u_2) - D(\frac{1}{u_3}) - D(\frac{1}{u_4}) + D(u_5), \\
D(t_1) - D(\frac{1}{t_2}) + D(t_3) - D(\frac{1}{t_4}) &= D(u_1) - D(\frac{1}{u_2}) - D(\frac{1}{u_3}) + D(u_4) - D(\frac{1}{u_5}), \\
D(t_1) - D(\frac{1}{t_2}) + D(t_3) - D(\frac{1}{t_4}) &= -D(\frac{1}{u_1}) - D(\frac{1}{u_2}) + D(u_3) + D(u_4) + D(u_5), \\
D(t_1) - D(\frac{1}{t_2}) + D(t_3) - D(\frac{1}{t_4}) &= -D(\frac{1}{u_1}) + D(u_2) + D(u_3) - D(\frac{1}{u_4}) - D(\frac{1}{u_5}),
\end{aligned}
$$

respectively by the definition of D and (18). Each of these identities are equivalent to (19) by the well-known fact $D(\frac{1}{z}) = -D(z)$, so the imaginary parts of (20), (21), (22), (23) hold. On the other hand, (20), (21), (22), (23) are analytic functions on certain 3-dimensional open set, so the real parts also hold up to some real constants. After evaluating $t_1 = t_2 = t_3 = t_4 = u_1 = u_2 = u_3 = u_4 = i$ and $u_5 = -1$ to these functions,[12] we find that all constants are zero.

Now assume the edge CD is collapsed to a point. Then we obtain the following relations.

$$
\begin{cases} u_1 = t_1' t_4'', \\ u_2 = t_1' t_2'', \end{cases}
\begin{cases} t_1 = u_1'' u_2'', \\ t_2 = u_1 u_2', \\ t_4 = u_1' u_2, \\ t_1 t_2 t_4 = 1. \end{cases} \tag{28}
$$

[12] Note that $\mathrm{Li}_2(-1) = -\frac{\pi^2}{12}$.

After the direct calculation of the imaginary part of (24), it coincides with

$$D(t_1) - D(\frac{1}{t_2}) - D(\frac{1}{t_4}) = D(u_1) + D(u_2)$$

by (28), and it holds by the additivity of volume. Because of the analyticity of (24) on certain 2-dimensional open set, the real part of (24) also holds up to a real constant. Evaluating $t_1 = t_2 = t_4 = \exp(\frac{2\pi i}{3})$ and $u_1 = u_2 = \exp(\frac{\pi i}{3})$ shows the constant is zero, so the identity (24) is true. Other identities (25), (26), (27) can be proved by the same method.

□

Now we prove the theorem by the calculation on each crossing n. At first, consider the case that no edge of the octahedron on the positive crossing n is collapsed. Let the variables assigned to the contributing sides be $z_a, \ldots, z_d$ as in Figure 9 and let $t_1 = \frac{z_b}{z_a}$, $t_2 = \frac{z_c}{z_b}$, $t_3 = \frac{z_d}{z_c}$, $t_4 = \frac{z_a}{z_d}$ as in Figure 10(a). Then the Yokota potential function of the crossing becomes

$$X(z_a, \ldots, z_d) := \mathrm{Li}_2(t_1) - \mathrm{Li}_2(\frac{1}{t_2}) + \mathrm{Li}_2(t_3) - \mathrm{Li}_2(\frac{1}{t_4})$$

and

$$\begin{aligned} X_0(z_a, \ldots, z_d) = {} & \mathrm{Li}_2(t_1) - \mathrm{Li}_2(\frac{1}{t_2}) + \mathrm{Li}_2(t_3) - \mathrm{Li}_2(\frac{1}{t_4}) \\ & + \left(-\log(1-t_1) + \log(1-\frac{1}{t_4})\right)\log z_a - \left(-\log(1-t_1) + \log(1-\frac{1}{t_2})\right)\log z_b \\ & + \left(-\log(1-t_3) + \log(1-\frac{1}{t_2})\right)\log z_c - \left(-\log(1-t_3) + \log(1-\frac{1}{t_4})\right)\log z_d. \end{aligned} \tag{29}$$

Likewise, let the variables assigned to the regions be $r_j, \ldots, r_m$ as in Figure 9 and let $u_1 = \frac{w_m}{w_j}$, $u_2 = \frac{w_k}{w_j}$, $u_3 = \frac{w_k}{w_l}$, $u_4 = \frac{w_m}{w_l}$, $u_5 = \frac{w_j w_l}{w_k w_m}$ as in Figure 10(a). Then the potential function of the colored Jones invariant of the crossing becomes P_f, which was defined in Lemma 3.1 for $f = 1, \ldots, 4$, and

$$\begin{aligned} P_{10} = {} & -\mathrm{Li}_2(u_1) - \mathrm{Li}_2(u_2) + \mathrm{Li}_2(\frac{1}{u_3}) + \mathrm{Li}_2(\frac{1}{u_4}) - \mathrm{Li}_2(u_5) + \frac{\pi^2}{6} - \log u_1 \log u_2 \\ & - (-\log(1-u_1) - \log(1-u_2) + \log(1-u_5) + \log u_1 + \log u_2)\log w_j \\ & - \left(\log(1-u_2) + \log(1-\frac{1}{u_3}) - \log(1-u_5) - \log u_1\right)\log w_k \\ & - \left(-\log(1-\frac{1}{u_3}) - \log(1-\frac{1}{u_4}) + \log(1-u_5)\right)\log w_l \\ & - \left(\log(1-u_1) + \log(1-\frac{1}{u_4}) - \log(1-u_5) - \log u_2\right)\log w_m. \end{aligned} \tag{30}$$

Assume $z_a, \ldots, z_d, w_j, \ldots, w_m$ satisfy the assumption of Lemma 5.1.[13] Let

$$\begin{cases} U_1 := -\log(1-t_1) + \log(1-\frac{1}{t_4}), \\ U_2 := -\log(1-t_1) + \log(1-\frac{1}{t_2}), \\ U_3 := -\log(1-t_3) + \log(1-\frac{1}{t_2}), \\ U_4 := -\log(1-t_3) + \log(1-\frac{1}{t_4}), \end{cases}$$

$$\begin{cases} T_1 := \log(1-u_1) + \log(1-u_2) - \log(1-u_5) - \log u_1 - \log u_2, \\ T_2 := -\log(1-u_2) - \log(1-\frac{1}{u_3}) + \log(1-u_5) + \log u_1, \\ T_3 := \log(1-\frac{1}{u_3}) + \log(1-\frac{1}{u_4}) - \log(1-u_5), \\ T_4 := -\log(1-u_1) - \log(1-\frac{1}{u_4}) + \log(1-u_5) + \log u_2. \end{cases}$$

Then, by (18),

$$\begin{cases} U_1 \equiv \log u_1 \equiv \log w_m - \log w_j \pmod{2\pi i}, \\ U_2 \equiv \log u_2 \equiv \log w_k - \log w_j \pmod{2\pi i}, \\ U_3 \equiv \log u_3 \equiv \log w_k - \log w_l \pmod{2\pi i}, \\ U_4 \equiv \log u_4 \equiv \log w_m - \log w_l \pmod{2\pi i}, \end{cases} \quad \begin{cases} T_1 \equiv \log t_1 \equiv \log z_b - \log z_a \pmod{2\pi i}, \\ T_2 \equiv \log t_2 \equiv \log z_c - \log z_b \pmod{2\pi i}, \\ T_3 \equiv \log t_3 \equiv \log z_d - \log z_c \pmod{2\pi i}, \\ T_4 \equiv \log t_4 \equiv \log z_a - \log z_d \pmod{2\pi i}, \end{cases}$$

and $U_1 + U_3 = U_2 + U_4$, $T_1 + T_2 + T_3 + T_4 = 0$. Applying these and (20) to (29) and (30), we obtain the remaining term Z_n of the crossing n as follows.

$$\begin{aligned} Z_n &:= X_0 + P_{10} = U_1 \log z_a - U_2 \log z_b + U_3 \log z_c - U_4 \log z_d \\ &\quad + T_1 \log w_j + T_2 \log w_k + T_3 \log w_l + T_4 \log w_m - U_1 \log u_2 - U_2 \log u_1 \\ &\quad + U_1 \log(1-u_1) + U_2 \log(1-u_2) + U_3 \log(1-\frac{1}{u_3}) + U_4 \log(1-\frac{1}{u_4}) - (U_1+U_3)\log(1-u_5) \\ &= T_1 \log w_j + T_2 \log w_k + T_3 \log w_l + T_4 \log w_m \\ &\quad + U_1 \left(\log z_a - \log z_d + \log(1-u_1) + \log(1-\frac{1}{u_4}) - \log(1-u_5) - \log u_2 \right) \\ &\quad + U_2 \left(-\log z_b + \log z_d + \log(1-u_2) - \log(1-\frac{1}{u_4}) - \log u_1 \right) \\ &\quad + U_3 \left(\log z_c - \log z_d + \log(1-\frac{1}{u_3}) + \log(1-\frac{1}{u_4}) - \log(1-u_5) \right) \\ &= T_2(\log w_k - \log w_j) + T_3(\log w_l - \log w_j) + T_4(\log w_m - \log w_j) \\ &\quad + U_1 (\log z_a - \log z_d - T_4) + U_2 (-\log z_b + \log z_d - T_2 - T_3) + U_3 (\log z_c - \log z_d + T_3) \\ &\equiv T_2(\log w_k - \log w_j) + T_3(\log w_l - \log w_j) + T_4(\log w_m - \log w_j) \\ &\quad + (\log w_m - \log w_j)(\log z_a - \log z_d - T_4) + (\log w_k - \log w_j)(-\log z_b + \log z_d - T_2 - T_3) \\ &\quad + (\log w_k - \log w_l)(\log z_c - \log z_d + T_3) \qquad \pmod{4\pi^2} \\ &= -(\log w_j - \log w_m)\log z_a - (\log w_k - \log w_j)\log z_b + (\log w_k - \log w_l)\log z_c \\ &\quad + (\log w_l - \log w_m)\log z_d. \end{aligned}$$

[13] Any essential solutions $(z_a, \ldots, z_d)$ of $\mathcal{H}_1$ and the corresponding essential solution $(w_j, \ldots, w_m)$ of $\mathcal{H}_2$ satisfy this assumption.

By the same method, we can prove that the remaining term of the negative crossing in Figure 9 is the same with that of the positive crossing.

Now we consider the case that only one horizontal edge is collapsed in an octahedron on a positive crossing n. Let the region assigned to r_l be an unbounded region and $z_c = z_d = 1$ in Figure 9. Also let $t_1 = \frac{z_b}{z_a}$, $t_2 = \frac{1}{z_b}$, $t_4 = z_a$ and $u_1 = \frac{w_m}{w_j}$, $u_2 = \frac{w_k}{w_j}$. Then the Yokota potential function of the crossing becomes

$$X(z_a, z_b) := \mathrm{Li}_2(t_1) - \mathrm{Li}_2(\frac{1}{t_2}) - \mathrm{Li}_2(\frac{1}{t_4}) + \frac{\pi^2}{6}$$

and

$$\begin{aligned} X_0(z_a, z_b) = &\ \mathrm{Li}_2(t_1) - \mathrm{Li}_2(\frac{1}{t_2}) - \mathrm{Li}_2(\frac{1}{t_4}) + \frac{\pi^2}{6} \\ &+ \left(-\log(1-t_1) + \log(1-\frac{1}{t_4})\right)\log z_a - \left(-\log(1-t_1) + \log(1-\frac{1}{t_2})\right)\log z_b. \end{aligned} \tag{31}$$

The potential function of the colored Jones invariant of the crossing becomes

$$Y(w_j, w_k, w_m) := P_1(w_j, w_k, 0, w_m) = -\mathrm{Li}_2(u_1) - \mathrm{Li}_2(u_2) + \frac{\pi^2}{6} - \log u_1 \log u_2$$

and

$$\begin{aligned} Y_0(w_j, w_k, w_m) = &-\mathrm{Li}_2(u_1) - \mathrm{Li}_2(u_2) + \frac{\pi^2}{6} - \log u_1 \log u_2 \\ &-(-\log(1-u_1) - \log(1-u_2) + \log u_1 + \log u_2)\log w_j \\ &-(\log(1-u_2) - \log u_1)\log w_k - (\log(1-u_1) - \log u_2)\log w_m. \end{aligned} \tag{32}$$

In this case, let

$$\begin{cases} U_1 := -\log(1-t_1) + \log(1-\frac{1}{t_4}), \\ U_2 := -\log(1-t_1) + \log(1-\frac{1}{t_2}), \end{cases}$$

$$\begin{cases} T_1 := \log(1-u_1) + \log(1-u_2) - \log u_1 - \log u_2, \\ T_2 := -\log(1-u_2) + \log u_1, \\ T_4 := -\log(1-u_1) + \log u_2. \end{cases}$$

Then, by (28),

$$\begin{cases} U_1 \equiv \log u_1 \equiv \log w_m - \log w_j \pmod{2\pi i}, \\ U_2 \equiv \log u_2 \equiv \log w_k - \log w_j \pmod{2\pi i}, \end{cases} \quad \begin{cases} T_1 \equiv \log t_1 \equiv \log z_b - \log z_a \pmod{2\pi i}, \\ T_2 \equiv \log t_2 \equiv -\log z_b \pmod{2\pi i}, \\ T_4 \equiv \log t_4 \equiv \log z_a \pmod{2\pi i}, \end{cases}$$

and $T_1 + T_2 + T_4 = 0$. Applying these and (24) to (31) and (32), we obtain the remaining term Z_n of the crossing n as follows.

$$\begin{aligned} Z_n \ := &\ X_0 + Y_0 = U_1 \log z_a - U_2 \log z_b + T_1 \log w_j + T_2 \log w_k + T_4 \log w_m - U_1 T_4 - U_2 T_2 \\ = &\ U_1 \log z_a - U_2 \log z_b + T_2(\log w_k - \log w_j - U_2) + T_4(\log w_m - \log w_j - U_1) \\ \equiv &\ U_1 \log z_a - U_2 \log z_b \\ &- \log z_b(\log w_k - \log w_j - U_2) + \log z_a(\log w_m - \log w_j - U_1) \pmod{4\pi^2} \\ = &-(\log w_j - \log w_m)\log z_a - (\log w_k - \log w_j)\log z_b. \end{aligned}$$

By the same method, we can prove the remaining term of the negative crossing in this case is the same with that of the positive crossing. On the other hand, the remaining term becomes

$$Z_n = -(\log w_k - \log w_j)\log z_b + (\log w_k - \log w_l)\log z_c$$

when the region assigned to r_m is an unbounded region,

$$Z_n = (\log w_k - \log w_l)\log z_c + (\log w_l - \log w_m)\log z_d$$

when the region assigned to r_j is an unbounded region, and

$$Z_n = -(\log w_j - \log w_m)\log z_a + (\log w_l - \log w_m)\log z_d$$

when the region assigned to r_k is an unbounded region.

Now we consider the case that the crossing point n is the endpoint of I or J. There are four cases as in Figure 19. We only prove the case of Figure 19(a) because the others can be proved by the same method.

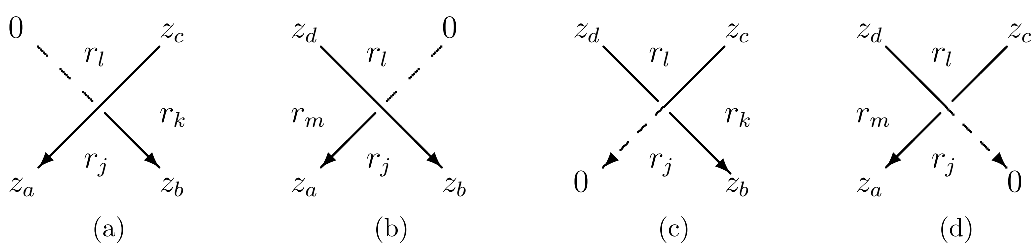

Figure 19: Four cases of the end point of I or J

At first, assume all three regions in Figure 19(a) are bounded. Then, in Figure 10(a), the edge $\mathrm{D}_n\mathrm{E}_n$ is collapsed to a point and $\frac{z_b}{z_a}$, $\frac{z_c}{z_b}$, $\frac{w_l}{w_j}$, $\frac{w_k}{w_l}$ are assigned to the edges $\mathrm{A}_n\mathrm{B}_n$, $\mathrm{B}_n\mathrm{C}_n$, $\mathrm{A}_n\mathrm{F}_n$, $\mathrm{C}_n\mathrm{F}_n$ respectively. Also we obtain

$$\frac{z_b}{z_a} = \left(\frac{w_l}{w_j}\right)'' = 1 - \frac{w_j}{w_l} \quad \text{and} \quad \frac{w_k}{w_l} = \left(\frac{z_c}{z_b}\right)'' = 1 - \frac{z_b}{z_c}. \tag{33}$$

Applying (33) to Yokota potential function $X(z_a, z_b, z_c) := \mathrm{Li}_2(\frac{z_b}{z_a}) - \mathrm{Li}_2(\frac{z_b}{z_c})$, we obtain

$$\begin{aligned} X_0 &= \mathrm{Li}_2(\frac{z_b}{z_a}) - \mathrm{Li}_2(\frac{z_b}{z_c}) - \log(1 - \frac{z_b}{z_a})\log z_a \\ &\quad - \left(-\log(1 - \frac{z_b}{z_a}) + \log(1 - \frac{z_b}{z_c})\right)\log z_b + \log(1 - \frac{z_b}{z_c})\log z_c \\ &= \mathrm{Li}_2(\frac{z_b}{z_a}) - \mathrm{Li}_2(1 - \frac{w_k}{w_l}) + \log\frac{w_j}{w_l}(\log z_b - \log z_a) + \log\frac{w_k}{w_l}(\log z_c - \log z_b). \end{aligned}$$

Also, applying (33) to the potential function of the colored Jones invariant $Y(w_j, w_k, w_l) := I_1(w_j, w_k, w_l) = -\mathrm{Li}_2(\frac{w_k}{w_l}) + \mathrm{Li}_2(\frac{w_j}{w_l})$, we obtain

$$\begin{aligned}
Y_0 &= -\mathrm{Li}_2(\frac{w_k}{w_l}) + \mathrm{Li}_2(\frac{w_j}{w_l}) + \log(1 - \frac{w_j}{w_l}) \log w_j \\
&\quad - \log(1 - \frac{w_k}{w_l}) \log w_k - \left(- \log(1 - \frac{w_k}{w_l}) + \log(1 - \frac{w_j}{w_l}) \right) \log w_l \\
&= -\mathrm{Li}_2(\frac{w_k}{w_l}) + \mathrm{Li}_2(1 - \frac{z_b}{z_a}) + \log \frac{z_b}{z_a}(\log w_j - \log w_l) + \log \frac{z_b}{z_c}(\log w_l - \log w_k).
\end{aligned}$$

Using the well-known identity $\mathrm{Li}_2(z) + \mathrm{Li}_2(1-z) = \frac{\pi^2}{6} - \log z \log(1-z)$ for $z \in \mathbb{C} - \{0, 1\}$ in [6], we obtain the remaining term

$$\begin{aligned}
Z_n \quad := \quad & X_0 + Y_0 = - \log \frac{z_b}{z_a} \log \frac{w_j}{w_l} + \log \frac{w_k}{w_l} \log \frac{z_b}{z_c} \\
& + \log \frac{w_j}{w_l}(\log z_b - \log z_a) + \log \frac{w_k}{w_l}(\log z_c - \log z_b) \\
& + \log \frac{z_b}{z_a}(\log w_j - \log w_l) + \log \frac{z_b}{z_c}(\log w_l - \log w_k) \\
= \quad & \log \frac{w_j}{w_l} \left(- \log \frac{z_b}{z_a} + \log z_b - \log z_a \right) + \log \frac{w_k}{w_l} \left(\log \frac{z_b}{z_c} + \log z_c - \log z_b \right) \\
& + \log \frac{z_b}{z_a}(\log w_j - \log w_l) + \log \frac{z_b}{z_c}(\log w_l - \log w_k) \\
\equiv \quad & (\log w_j - \log w_l) \left(- \log \frac{z_b}{z_a} + \log z_b - \log z_a \right) \\
& + (\log w_k - \log w_l) \left(\log \frac{z_b}{z_c} + \log z_c - \log z_b \right) \\
& + \log \frac{z_b}{z_a}(\log w_j - \log w_l) + \log \frac{z_b}{z_c}(\log w_l - \log w_k) \pmod{4\pi^2} \\
= \quad & -(\log w_j - \log w_l) \log z_a - (\log w_k - \log w_j) \log z_b + (\log w_k - \log w_l) \log z_c.
\end{aligned}$$

Finally we consider the case that the region assigned with r_j in Figure 19(a) is unbounded. Then the edges $\mathrm{D}_n\mathrm{E}_n$ and $\mathrm{A}_n\mathrm{B}_n$ are collapsed to points. Furthermore, $z_a = z_b = 1$ and $w_j = 0$, and z_c, $\frac{w_k}{w_l}$ are assigned to the edges $\mathrm{B}_n\mathrm{C}_n$, $\mathrm{C}_n\mathrm{F}_n$ in Figure 10(a) respectively. Applying

$$\frac{w_k}{w_l} = z_c'' = 1 - \frac{1}{z_c}$$

to Yokota potential function $X(z_c) := -\mathrm{Li}_2(\frac{1}{z_c}) + \frac{\pi^2}{6}$, we obtain

$$X_0 = -\mathrm{Li}_2(\frac{1}{z_c}) + \frac{\pi^2}{6} + \log(1 - \frac{1}{z_c}) \log z_c = -\mathrm{Li}_2(\frac{1}{z_c}) + \frac{\pi^2}{6} + \log \frac{w_k}{w_l} \log z_c,$$

and to the potential function of the colored Jones invariant $Y(w_k, w_l) := I_1(0, w_k, w_l) = -\mathrm{Li}_2(\frac{w_k}{w_l})$, we obtain

$$Y_0 = -\mathrm{Li}_2(\frac{w_k}{w_l}) - \log(1 - \frac{w_k}{w_l})(\log w_k - \log w_l) = -\mathrm{Li}_2(1 - \frac{1}{z_c}) - \log \frac{1}{z_c}(\log w_k - \log w_l).$$

Therefore, we obtain the remaining term

$$\begin{aligned} Z_n &:= X_0 + Y_0 = \log\frac{1}{z_c}\log\frac{w_k}{w_l} + \log\frac{w_k}{w_l}\log z_c - \log\frac{1}{z_c}(\log w_k - \log w_l) \\ &= \log\frac{1}{z_c}(\log\frac{w_k}{w_l} - \log w_k + \log w_l) + \log\frac{w_k}{w_l}\log z_c \\ &\equiv -\log z_c(\log\frac{w_k}{w_l} - \log w_k + \log w_l) + \log\frac{w_k}{w_l}\log z_c \pmod{4\pi^2} \\ &= (\log w_k - \log w_l)\log z_c. \end{aligned}$$

Likewise, we can show the remaining term becomes

$$Z_n = -(\log w_j - \log w_l)\log z_a$$

when the region assigned to r_k in Figure 19(a) is unbounded, and other three cases in Figure 19 can be obtained by the same method.

Finally note that

$$\sum_{n\,:\,\text{crossings of }G} Z_n = 0,$$

because, for a contributing side with z_a in Figure 9, if the side goes out of the crossing point, then the coefficient of $\log z_a$ is $-(\log w_j - \log w_l)$, and if the side goes into the crossing point, then the coefficient of $\log z_a$ is $(\log w_j - \log w_l)$. They are cancelled each other, and it happens for all the contributing sides, so we complete the proof.

Acknowledgments The authors show gratitude to Yoshiyuki Yokota for sending us his preprint in advance before publication. The first author is supported by Grant-in-Aid for JSPS Fellows 21.09221.

References

[1] J. Cho. Yokota theory, the invariant trace fields of hyperbolic knots and the borel regulator map. http://arxiv.org/abs/1005.3094, 2010.

[2] J. Cho and J. Murakami. The complex volumes of twist knots via colored Jones polynomial. To appear in J. Knot Theory Ramifications.

[3] N. M. Dunfield. Cyclic surgery, degrees of maps of character curves, and volume rigidity for hyperbolic manifolds. *Invent. Math.*, 136(3):623–657, 1999.

[4] S. Francaviglia. Hyperbolic volume of representations of fundamental groups of cusped 3-manifolds. *Int. Math. Res. Not.*, (9):425–459, 2004.

[5] R. M. Kashaev. The hyperbolic volume of knots from the quantum dilogarithm. *Lett. Math. Phys.*, 39(3):269–275, 1997.

[6] L. Lewin, editor. *Structural properties of polylogarithms*, volume 37 of *Mathematical Surveys and Monographs*. American Mathematical Society, Providence, RI, 1991.

[7] R. Meyerhoff. Density of the Chern-Simons invariant for hyperbolic 3-manifolds. In *Low-dimensional topology and Kleinian groups (Coventry/Durham, 1984)*, volume 112 of *London Math. Soc. Lecture Note Ser.*, pages 217–239. Cambridge Univ. Press, Cambridge, 1986.

[8] H. Murakami. The asymptotic behavior of the colored jones function of a knot and its volume. *Proceedings of 'Art of Low Dimensional Topology VI', edited by T. Kohno, January*, 2000.

[9] H. Murakami. Optimistic calculations about the Witten-Reshetikhin-Turaev invariants of closed three-manifolds obtained from the figure-eight knot by integral Dehn surgeries. *Sūrikaisekikenkyūsho Kōkyūroku*, (1172):70–79, 2000. Recent progress towards the volume conjecture (Japanese) (Kyoto, 2000).

[10] H. Murakami. Kashaev's invariant and the volume of a hyperbolic knot after Y. Yokota. In *Physics and combinatorics 1999 (Nagoya)*, pages 244–272. World Sci. Publ., River Edge, NJ, 2001.

[11] H. Murakami and J. Murakami. The colored Jones polynomials and the simplicial volume of a knot. *Acta Math.*, 186(1):85–104, 2001.

[12] H. Murakami, J. Murakami, M. Okamoto, T. Takata, and Y. Yokota. Kashaev's conjecture and the Chern-Simons invariants of knots and links. *Experiment. Math.*, 11(3):427–435, 2002.

[13] K. Ohnuki. The colored Jones polynomials of 2-bridge link and hyperbolicity equations of its complements. *J. Knot Theory Ramifications*, 14(6):751–771, 2005.

[14] D. Thurston. Hyperbolic volume and the jones polynomial. Lecture note at "Invariants des noeuds et de variétés de dimension 3", available at http://www.math.columbia.edu/˜dpt/speaking/Grenoble.pdf, June 1999.

[15] W. Thurston. The geometry and topology of three-manifolds. Lecture Note. available at http://www.msri.org/publications/books/gt3m/.

[16] S. Tillmann. Degenerations of ideal hyperbolic triangulations. http://arxiv.org/abs/math/0508295.

[17] V. G. Turaev. The Yang-Baxter equation and invariants of links. *Invent. Math.*, 92(3):527–553, 1988.

[18] J. Weeks. Computation of hyperbolic structures in knot theory. In *Handbook of knot theory*, pages 461–480. Elsevier B. V., Amsterdam, 2005.

[19] Y. Yokota. On the complex volume of hyperbolic knots. To appear in J. Knot Theory Ramifications.

[20] Y. Yokota. On the volume conjecture for hyperbolic knots. http://arxiv.org/abs/math/0009165.

[21] C. K. Zickert. The volume and Chern-Simons invariant of a representation. *Duke Math. J.*, 150(3):489–532, 2009.

Department of Mathematics, Faculty of Science and Engineering, Waseda University, 3-4-1 Okubo, Shinjuku-ku, Tokyo 169-8555, Japan
E-mail: dol0425@gmail.com
murakami@waseda.jp